THE EFFECTS OF ER STRESS ON GLIAL CELLS: EVIDENCE FROM BOTH *IN VIVO* AND *IN VITRO* MODELS

A THESIS SUBMITTED TO

THE GRADUATE SCHOOL OF ENGINEERING AND SCIENCE

OF BİLKENT UNIVERSITY

IN PARTIAL FULFILLMENT OF THE REQUIREMENTS FOR

THE DEGREE OF

MASTER OF SCIENCE

IN

MATERIALS SCIENCE AND NANOTECHNOLOGY

By

Duygu Mutlu

January 2022

The Effects of ER Stress on Glial Cells: Evidence from Both *In Vivo* and *In Vitro* Models
By Duygu Mutlu
January 2022

We certify that we have read this thesis and that in our opinion it is fully adequate, in scope and in quality, as a thesis for the degree of Master of Science.

Michelle Adams(Advisor)

Ebru Erbay(Co-Advisor)

Özlen Konu Karakayalı

Çağdaş Devrim Son

Approved for the Graduate School of Engineering and Science:

Ezhan Karaşan
Director of the Graduate School

ABSTRACT

THE EFFECTS OF ER STRESS ON GLIAL CELLS: EVIDENCE FROM BOTH *IN VIVO* AND *IN VITRO* MODELS

Duygu Mutlu
M.S. in MATERIALS SCIENCE AND NANOTECHNOLOGY
Advisor: Michelle Adams
Co-Advisor: Ebru Erbay
January 2022

Consuming high fat diet for long periods of time increases neuroinflammation, which may result in cognitive decline and loss in memory formation. Excessive free fatty acid influx stresses the ER and mitochondria, two important organelles taking part in protein folding and energy production. The ER responds to stress in part by activating Protein Kinase RNA-like Endoplasmic Reticulum Kinase (PERK) pathway. It has been shown that PERK pathway activation inhibits mitophagy (autophagy of mitochondria) in macrophages. Since microglia are the immune cells of the Central Nervous System (CNS), first I investigated the effects of high fat diet in the cortex of wild type (C57BL/6) and ApoE -/- mice by looking at microglial marker Iba1. Western Blot analysis showed no significant effects of diet and genotype on Iba1 level. I also found that there is no correlation between Iba1 and GFAP (astrocyte marker) levels for these mice.

Brain contains many other types of cells and in order to effects of ER stress directly on the microglia, I moved on to the BV2 mouse microglial cell line. There were differential effects of ER stress induction with thapsigargin and palmitate treatments. An increase in ER stress markers such as CHOP and p-IRE1 αhas been observed with both treatments. While CHOP protein levels could not reach significance, there was an increasing numerical trend. p-IRE1 $\alpha$was marginally significant for both treatments (p=0.087 for thapsigargin and p=0.061 for 100 μM palmitate). Mitophagy indicators (Pink1 and p62) were assessed with Western Blot analysis after successful mitochondria isolation from BV2 cells. The data indicated that p62 marginally increased with both palmitate (p=0.61) and thapsigargin (p=0.1) treatments. Following both treatments, very subtle effects

of ER stress were observed. This suggests that further experiments examining optimal dosage and duration need to be performed. Overall, the induction of ER stress appears to induce mitophagy and alter microglia, which likely leads to altered cellular and synaptic function.

Keywords: High Fat Diet, Mitophagy, Microglia, ER Stress.

ÖZET

ER STRESIN GLIA HUCRELERI UZERINDEKI ETKISI: *IN VIVO* VE *IN VITRO* MODELLERDEN KANITLAR

Duygu Mutlu
Malzeme Bilimi ve Nanoteknoloji, Yüksek Lisans
Tez Danışmanı: Michelle Adams
İkinci Tez Danışmanı: Ebru Erbay
Ocak 2022

Uzun süre yüksek yağlı diyet tüketmek, nöroinflamasyonu artırır, bu da bilişsel gerlilemeye ve hafıza oluşumu kaybına yol açabilir. Serbest yağ asitlerinin birikmesi protein katlanması ve enerji üretiminde görev alan iki önemli organeli (ER ve mitokondri) strese sokar. ER, bu stres karşısında Protein Kinaz RNA benzeri Endoplazmik Retikulum Kinaz (PERK) yolağını aktive eder. PERK yolu aktivasyonunun makrofajlarda mitofajiyi (mitokondri otofajisi) inhibe ettiği gösterilmiştir. Mikroglia, Merkezi Sinir Sisteminin (CNS) bağışıklık hücreleri olduğundan, önce yüksek yağlı diyetin C57BL/6 ve ApoE -/- farelerin korteksindeki etkilerini mikroglial işaretleyici Iba1'e bakarak araştırdım. Western Blot analizi, diyet ve genotipin Iba1 seviyesi üzerinde önemli bir etkisi olmadığını gösterdi. Ayrıca bu fareler için Iba1 ve GFAP (astrosit belirteci) seviyeleri arasında bir korelasyon olmadığını buldum.

Beyin bir çok farklı hücre tipi içerdiğinden, ER stresinin etkilerini direkt olarak mikroglia üzerinde görmek için BV2 fare mikroglial hücre hattına geçtim. Thapsigargin ve palmitat tedavileri ile ER stres indüksiyonunun farklı etkileri gözlendi. Her iki tedavide de CHOP ve p-IRE1 αgibi ER stres belirteçlerinde bir artış gözlemlendi. CHOP protein seviyeleri anlamlılığa ulaşamazken, artan bir sayısal eğilim olduğu belirlendi. p-IRE1 α, her iki tedavi için de marjinal olarak anlamlıydı (tapsigargin için p=0.087 ve 100 μM palmitat için p=0.061). BV2 hücrelerinden başarılı bir şekilde mitokondri izole edildikten sonra mitofaji indikatörleri (Pink1 ve p62) Western Blot analizi ile değerlendirildi. Alınan sonuçlar, p62'nin hem palmitat (p=0.61) hem de thapsigargin (p=0.1) tedavileri ile marjinal olarak arttığını gösterdi. Her iki tedaviyi takiben, ER stresinin

hafif etkileri gözlemlendi. Bu, optimal dozaj ve süreyi inceleyen başka deneylerin yapılması gerektiğini göstermektedir. Genel olarak, ER stresinin uyarılmasının mitofajiyi indüklediği ve mikrogliayı değiştirdiği, aynı zamanda hücresel ve sinaptik fonksiyonda değişikliğe yol açabileceği görülmektedir.

Anahtar sözcükler: Yüksek yağlı diyet, Mitofaji, Mikroglia, ER stresi.

Acknowledgement

I would like to thank my advisors; Prof. Michelle Marie Adams and Assoc. Prof. Ebru Erbay for always inspiring me to chase critical thinking and providing me with the tools to improve myself. I am grateful for my thesis defence committee Assoc. Prof. Özlen Konu Karakayalı and Assoc. Prof. Çağdaş Devrim Son for their time and efforts to improve this thesis. I acknowledge Dr.Güneş Özhan Baykan and her lab (Izmir Biomedicine and Genome Center) for providing the BV2 cell line.

Every present and past member of Adams lab offered their help and friendship through out my master's degree; Narin Ilgım Ardıç, Serena Sevdiye Aktürk, Dr. Begün Erbaba, Dr. Elif Tuğçe Karoğlu-Eravşar, Duygu Macaroğlu, Dr. Ergül Dilan Çelebi-Birand, Hande Özge Aydoğan, Dr. Melek Umay Tüz-Şaşik, Büşranur Şeker, Ece Avcı, İrem İnel and Fulya Kızıldağ. I want to especially thank Naz Mengi and Bilge Aşkın, who first welcomed me into the Adams Lab and showed me how to find my way around, in addition to being great mentors. Beyza Özen is an excellent friend and a talented scientist, she entertained me with her intelligence while we spent many days and nights working in the lab.

I would like express my gratitude to Erbay lab; Dr.Umut İnci Onat, Dr. Hamid Muhammed Syed, Zehra Tatlı Yıldırım, Aslı Ekin Doğan, Zehra Veli and Dr. Kikkie Poels. Aslı Dilber Yıldırım has been a brilliant mentor to me, offering her guidance both in the lab and personal life.

Yeşim and Dr. Savaş Mutlu are the best parents that I could ever wish for, and without their unconditional love and support, I wouldn't be the person I am today. They deserve a diploma just for putting up with me.

Finally, my partner Berk Can Şavak, who always finds a way to make me laugh even in the hardest times. You overcome my pessimism with your loving and joyful character.

I would like to acknowledge Bilkent University for providing financial support for the experimental work and my scholarship.

Contents

List of Figures

List of Tables

Chapter 1

Introduction

1.1 Hyperlipidemia

Increase in western style diets (high in cholesterol/high in fat) has resulted in worldwide obesity crisis [1]. Consuming a high fat diet for a long-term can cause metabolic diseases such as atherosclerosis, hypertension, type 2 diabetes and non-alcoholic fatty liver disease [2] [3] [4]. In addition to the metabolic diseases, there is a growing literature on how this excessive fat intake induces neuroinflammation, which results in impaired memory formation and cognitive decline [5].

Feeding animals with high fat diet to induce inflammation and ER stress has been studied extensively in the literature [6] [7] [8] [9] [10], however to observe full effects of hyperlipidemia and simulate human conditions, a knock out model has been proposed [11]. Apolipoprotein E (ApoE) is a part of plasma 4 lipoproteins that binds to LDL receptors [12]. It is used in hypercholesterolaemia and atherosclerosis studies, since when these mice are fed with chow diet, cholesterol becomes four times the normal and with western diet, their cholesterol becomes twenty times the normal cholesterol of wild type C57BL/6 mice [13] [14]. Onat et al. showed that ApoE -/- mice fed with Western and Chow Diet is a suitable model to study the effects of ER stress and mitophagy [15]. Furthermore,

promising results have been obtained in non-neuronal tissues.

1.2 Microglia

Microglia arise from myeloid precursors in the yolk sac and constitute about 5% of the cells in the cortex and corpus callosum [16]. They are found in two states; ramified (resting) state and activated state (Figure 1.1). While in resting state, they express CD11b, F4/80, Fc-gamma receptor 1 (CD64), and CD115 (Csf-1R) and proto-oncogene tyrosine-protein kinase MER (MerTK) [17]. They are the first responders to cellular debris and pathogens since they circulate the brain to maintain homeostasis [18]. Once they encounter such damage, microglia become activated and start to secrete cytokines to induce inflammatory response [19]. Activated microglia takes amoeboidic shape to phagocyte any debris or pathogen, and upregulate CD45, CD80, CD11c, CD86, CD40 and most importantly major histocompatibility complex class II (MHCII) [17].

Ionized calcium-binding adapter molecule 1 (Iba-1) takes part in in phagocytosis by reorganizing actin with L-fimbrin [20]. It is often regarded as a pan-microglial marker (expressed in both active and resting microglia), however its expression increases with microglial activation [21]. It does not conclude the total number of microglia in a given tissue.

Astrocytes are another type of glial cells that exist in the CNS. They are characterized with Glial Fibrillary Acidic Protein (GFAP) expression [22]. Interesting part of their job is to synthesize cholesterol to neurons with the help of ApoE [23].

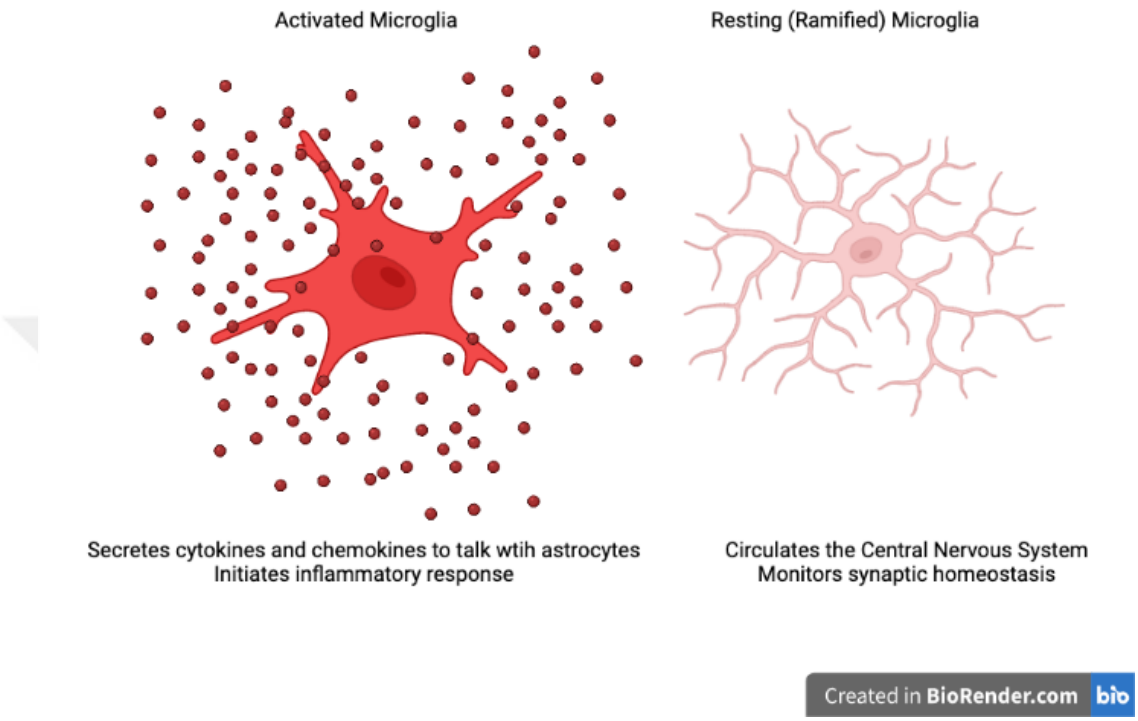

Figure 1.1: Activated vs Resting (Ramified) Microglia and their properties. This image is created with BioRender.com

1.2.0.1 BV2 Mouse Microglial Cell Line

BV2 cells were created by Blasi and colleagues by infecting female primary mouse microglial cell cultures with a v-raf/v-myc oncogene carrying retrovirus (J2) [24]. It is a well established mouse microglial cell line used in many studies including Alzheimer's Disease, G protein-coupled receptors and neuroinflammation [25] [26] [27]. Thus, BV2 cell line has proved itself as a reliable model to study microglia *in vitro*.

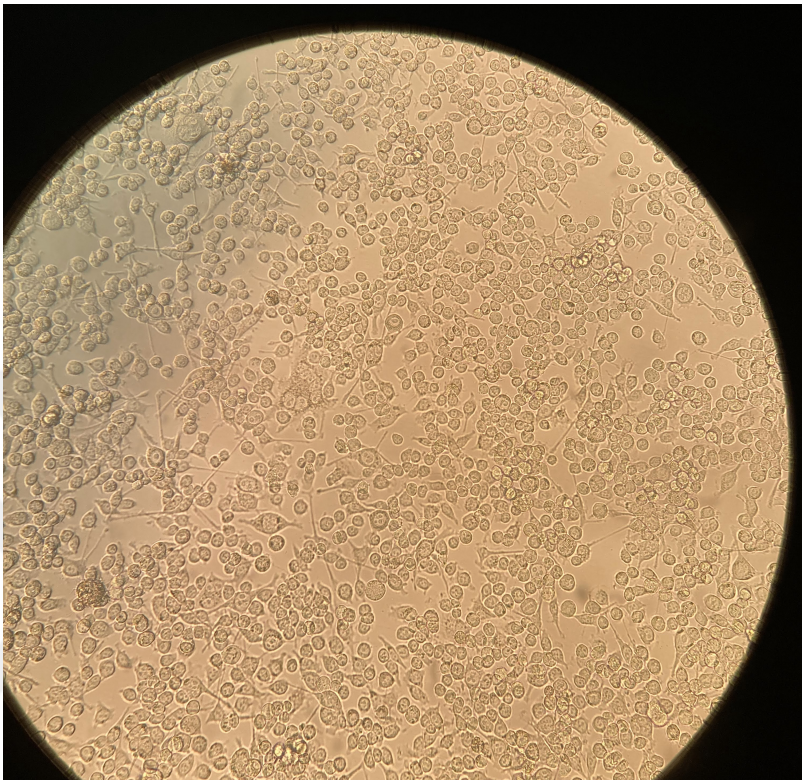

Figure 1.2: The microscopic image of BV2 cells, bright field, 20× magnification.

Image taken with Zeiss DIC equipped upright fluorescence microscope in Bilkent, UNAM.

1.3 Organelle Stress

1.3.1 ER stress

Endoplasmic reticulum (ER) consists of two compartments; rough part contains ribosomes for protein synthesis, and the smooth part synthesizes lipids. In addition to protein synthesis and folding, ER also stores and regulates calcium metabolism [28]. Having a role in so many vital processes, ER's function can be disturbed by external factors such as viruses, as well as internal factors like

oxidative stress, changes in calcium levels and abundant influx of fatty acids [29]. Under these conditions, misfolded proteins start to accumulate in the cells. To handle the stress; ER activates Unfolded Protein Response (UPR), consisting of three pathways; inositol-requiring-enzyme-1 (IRE1), protein kinase RNA (PKR) like ER kinase (PERK) and the activating transcription factor 6 (ATF6) (Figure 1.3) [30] [31]. PERK pathway activation causes global protein synthesis reduction, increased inflammatory cytokines, apoptotic markers upon activation[32]. In order to do that, PERK phosphorylates eukaryotic initiation factor 2 α(eIF2 α) at serine-51 to block protein translation except for Activating Transcription Factor 4 (ATF4). If the source of stress is not removed, apoptosis occurs through the inhibition of B-cell leukemia 2 (BCL-2) by C/EBP-homologous protein (CHOP) [33]. ATF4 also binds to Lon Protease 1 (LONP1) promoter to induce its expression which then degrades Pink1 (discussed in the next chapter) [34].

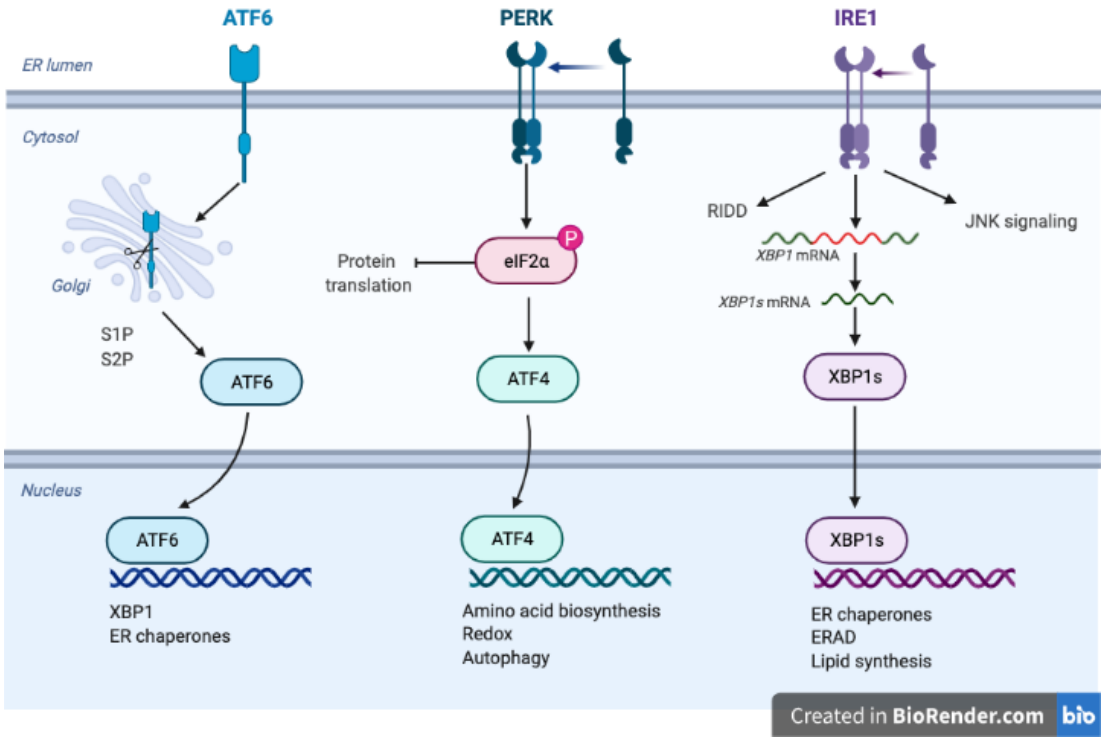

Figure 1.3: Unfolded Protein Response (UPR) of ER. This image is created with BioRender.com using Emma Madden's template.

1.3.1.1 Thapsigargin

Thapsigargin is a chemical toxin which depletes ER calcium stores by blocking intracellular Ca^{2+} ATPases [35]. The depletion of ER's calcium stores increases stress and activates PERK pathway. In this thesis, Thapsigargin is used to show PERK activation in BV2 cells.

1.3.2 Mitochondrial stress

Mitochondria are the vital organelles which produce adenosine triphosphate (ATP) by oxidative phosphorylation from glucose molecules [36]. They produce energy that is required for survival, which is especially important for brain cells since they have a high energy demand for synaptic neurotransmission, in addition to maintaining ion channels in the axonal, somatic, dendritic and presynaptic segments [37] [38]. Loss of energy would result in interruptions in neurotransmission, and eventually cognitive decline and neurodegenerative diseases. In the literature, studies found that there is mitochondria malfunctioning in many neurodegenerative diseases such as Alzheimer's Disease, Parkinson's Disease and Dementia [39] [40] [41] [42].

ER is connected to mitochondria through ER-mitochondria associated membrane (MAM) and PERK is found there [43]. When ER is stressed (mentioned in the previous section), it may release calcium (Ca^{2+}) into the mitochondria, causing depolarization of inner mitochondrial membrane [44]. Once the mitochondrial integrity is disrupted; mitochondria start to release cytochrome c into the cytosol together with reactive oxygen species (ROS), hydrogen peroxide (H_2O_2) and mitochondrial DNA (mtDNA). Cytochrome c further activates apoptotic genes [45]. Release of this particles further enhance the cellular oxidative stress and inflammatory response. So, the damaged mitochondria must be removed from the environment for the cells to function. They fuse with autophagosomes to be degraded by lysosomes in a process called mitophagy [46].

1.3.2.1 Mitophagy

Zheng et al., showed that mitophagy activation increases retrograde transport of axonal mitochondria, meaning that dysfunctional mitochondria is transported to soma of the neuron [47]. Mitophagy can occur in two ways; ubiquitin mediated or receptor mediated [48]. Receptor mediated pathway becomes active under hypoxic conditions [49]. In this pathway, NIX (NIP3-like protein X) binds to MAP1 light chain 3 (LC3) to induce merging mitochondria with lysosomes in the autophagosome complex with the help of adaptor proteins BCL2/adenovirus E1B 19 kDa protein interacting protein 3 (BNIP3) and FUN14 domain containing 1(FUNDC1) [49]. In the ubiquitin mediated pathway (also known as Pink1/Parkin pathway), serine/threonine PTEN-induced putative kinase 1 (PINK1) and Parkin are both associated with Alzheimer's Disease and Parkinson's Disease [50] [51]. Under normal conditions, after it is synthesized in the outer membrane of mitochondria, Pink1 is degraded by Lon Protease1 (LONP1) in the inner membrane of mitochondria, so it can not activate further cascades [52]. However, under stress conditions, it starts to accumulate in the place where it's synthesized, thus serving as a distress signal for mitophagy. In the inner membrane of mitochondria, it phosphorylates Parkin [53]. Once Parkin is activated, it ubiquitinates mitochondrial proteins such as; VDAC1, MFN1, MFN2, and Miro1 to isolate the dysfunctional mitochondria. After interacting with P62/sequestesome 1 (p62/SQSTM1) and optineurin, they form the autophagosome complex with LC3 to be degraded (Figure 1.4) [54].

Mitophagy regulation and PERK pathway is suggested to be one of the therapeutic strategies for many neurodegenerative diseases [55] [56].

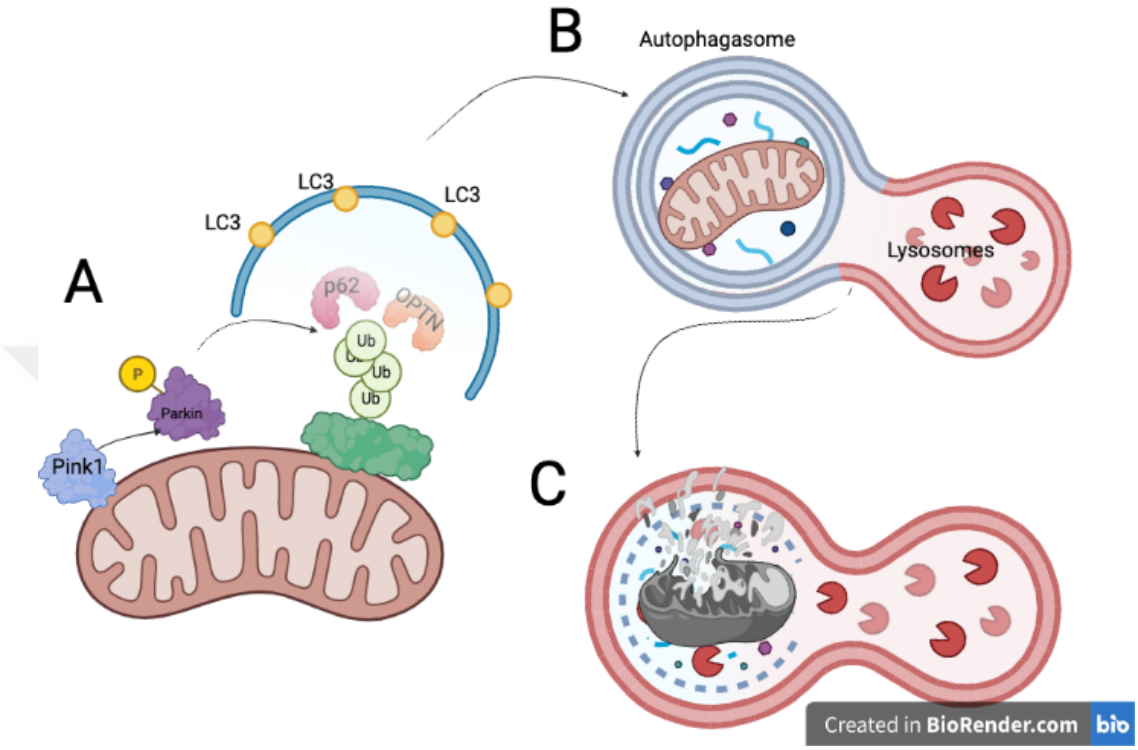

Figure 1.4: Mechanism of mitophagy. A. Pink1 is accumulated in the outer membrane of the mitochondrion. It phosphorylates Parkin, Parkin ubiqutinates other mitochondrial proteins, p62/sequestesome 1 and optineurin binds to these proteins. B. LC3 induces merging of mitochondrion and the autophagosome complex. C. Dysfunctional mitochondrion is degraded by lysosomes. This image is created with BioRender.com

1.3.2.2 Palmitate

Palmitate is a saturated fatty acid which can be easily directly incorporated into structural lipids in the brain without having being degraded to acetate first [57] [58]. It has important functions in membrane remodeling and synthesis, cell growth and the formation of myelin sheets around oligodendrocytes [59]. However, excessive palmitate causes mitochondrial stress by increasing the number of mitochondrial reactive oxygen species (mtROS), and shown to influence mitophagy in podoctyes [60] [61].

1.4 Aim of the Study

It has been shown that PERK pathway activation inhibits mitophagy in Bone Marrow Derived Macrophages, RAW264.7 cells [15], SH-SY5Y cells [62], and C57BL/6 mice [63]. So, it is logical to investigate the effects of high-fat diet induced organelle stress in the microglia, because they are the macrophages of the Central Nervous System. Also, microglia are highly susceptible to the changes in lipid metabolism and energy production, which makes them dependant on lipid synthesis and protein folding capacity of ER, and ATP production of mitochondria.

The hypothesis of this thesis is to examine if high fat diet increases ER stress, and then causing mitophagy inhibition in microglia. This was done in two models; first, an *in vivo* model using mice that have genetically high lipid levels in addition to being fed a diet high in cholesterol and then second, an *in vitro* model using a BV2 microglial cell line that had ER stress induced.

Chapter 2

Methods

The sections marked with an asterisk (*) were performed by Naz Mengi and Bilge Aşkın.

2.1 *Animals

The animals and procedures used in this thesis were approved by Bilkent animal ethical care committee (protocol no: 2018/2). The experiments were carried out in Bilkent Molecular Biology and Genetics Department and National Nanotechnology Research Center (UNAM), in collaboration with Prof. Dr. Michelle Adams and Prof. Dr. Ebru Erbay.

Genotype	Diet	Gender
C57BL/6	Chow Diet	Male (n=7)
C57BL/6	Western Diet	Male (n=7)
ApoE -/-	Chow Diet	Male (n=7)
ApoE -/-	Western Diet	Male (n=7)

Table 2.1: Genotype, Diet and Gender of the mice used in this thesis

The mice stated above were purchased from Charles River, Wilmington, Massachusetts. They were maintained at 22°C, 45% humidity, 12 hour light/dark cycle in Bilkent Animal Facility. Starting from 9 weeks old, they started Chow (4.5% fat) or Western diet (0.21% cholesterol, 21% butterfat, catalog: TD.88137 E15721, Ssniff Spezialdiaten, Germany) for 16 weeks.

2.1.1 *Dissection

At the end of 16 weeks of diet, the mice were anesthetized and then sacrificed by intraperitoneal injection of xylazine (10 mg/kg) and ketamine (100 mg/kg) mix. After couple of minutes, the mice were examined for the presence of any reflexes. Once the reflexes were completely gone, the abdominal cavity was cut open, 10 ml of PBS was injected to the heart to wash out the blood from internal organs and brain. After declaring animals dead; they were decapitated and brains were extracted on an ice cold petri dish. The olfactory bulb and cerebellum were cut off, then hippocampi were dissociated from cortex. Finally, all tissues were snap frozen until further experiments in liquid nitrogen.

2.1.2 *Tissue Homogenization and Protein Isolation

5 ml Homogenization Buffer (recipe given in Table 2.4) was completed by adding 50 μl PI, 50 μl PIC, 50 μl PMSF and 50 μl Sodium Orthovanadate. Each cortex was mechanically homogenized with a glass douncer containing 1 ml Homogenization Buffer, then centrifuged at 8000 g for 6 minutes. The supernatant was removed as much as possible and pellet was dissolved in 1 ml RIPA Buffer (Table 2.5) followed by a sonication for 6 times, each 1 minute. After 30 minutes incubation on ice, 13000 rpm 20 minutes centrifugation took place. Finally, supernatant was stored at -80°C for further experiments.

2.2 Cell Culture

Murine microglial cells BV2 cell line was kindly provided by Dr. Güneş Özhan Baykan (Izmir Biomedicine and Genome Center) and her students. They were cultured using methods described in [64].

Dulbecco's modified Eagle's medium (DMEM) was completed by addition of heat inactivated 10% Fetal Bovine Serum (FBS), 1% Penicillin-Streptomycin and 1% L-Glutamine. The cells were cultured when they reach 70-80% of confluency in an incubator fixed at 37°C 5% CO_2. For all of the experiments the cells were seeded at $5x10^6$ density on 6 well plates.

2.2.1 Thapsigargin Treatment

Thapsigargin treatment was done by the methods described in [65]. First, BV2 cells received 1 μM and 2 μM Thapsigargin in complete DMEM or DMSO as control. Then, after observing significant cell death, the concentration was decreased to 200 nM. After 24 hours; cells were washed with room temperature PBS, and then collected for RNA and mitochondria isolation.

2.2.2 Palmitate Treatment

For the palmitate treatment, the dosage was first determined to be 250 μM and 500 μM for 16 hours. However there was no change in ER stress and mitophagy markers, so the dosages were reduced to 100 μM and 200 μM for 24 hours, as explained in [66]. Palmitate was dissolved in the DMEM containing 1% fatty acid free Bovine Serum Albumin (BSA) heated to 65°C for 15 minutes, then given to the cells once it reached 37°C, ethanol was given to the BV2 cells as control for 24 hours. Afterwards, cells were washed with PBS and collected for further experiments.

2.2.3 Mitochondria Isolation

In order to isolate mitochondria from the BV2 cells; 120 μl Phospholysis Buffer (Table 2.6) was added to each well of the 6 well plate. After resting on ice for 5 minutes, the cells were collected into eppendorf tubes and homogenized 7 times using a 27.5 g needle. The homogenates were then centrifuged at 600 g for 5 minutes. 50 μl of the supernatant was labeled as Whole Cell Lysate, rest was transferred to a new eppendorf and then centrifuged for 10 minutes at 7000 g. Supernatant was labeled as Cyto fraction, and the pellet was resuspended with 50 μl of Phospholysis Buffer. It was then centrifuged for 5 minutes at 7000 g and pellet was resuspended with Phospholysis Buffer. This process was repeated two times. Finally, the Mitochondria pellet was resuspended with 35 μl of Phospholysis Buffer. All fractions were stored at -80°C until used for rest of the experiments.

2.3 DC Assay

DC Assay was performed to assess protein quantification. BSA ranging from 0 μg /ml to 1 μg / ml was used to prepare a standard curve to determine the unknown protein concentration based on the absorbance levels. Blank included only dH_2O. All of the sample proteins, BSA concentrations and blank has been loaded to a 96 well plate. Each well received 25 μl of Reagent A and Reagent S mixture (which was prepared by adding 20 μl Reagent S to each 1 ml of Reagent A), and 200 μl of Reagent B. Then the plate was left in the dark for 15 min for incubation. After mixing the 96 well plate, the wells were read by multi-plate reader (SpectraMax M5, Molecular Devices, Sunnyvale, CA, USA) at 650 nM. All of the concentrations and the standard curve can be found in Table 2.3 and Figure 2.1, respectively. The unknown sample concentrations were calculated according to equation of the linear fit. Later on, brain samples were equalized to 40 μg using water and 2x dye. Meanwhile, Whole Cell Lysate and Cyto samples were equalized to 35 μg and Mito samples to 7 μg using Phospholysis Buffer and

4x dye (Table 2.14). All protein samples were heated to 95°C for 5 minutes and stored at -80°C for the upcoming experiments.

2.4 Western Blot

2.4.1 Gel and Sample Preparation, Running

Firstly, 1 M Tris-HCl pH 8.8 and 1 M Tris-HCl pH 6.8 were prepared by dissolving 48 g of Tris base into 400 ml of dH_2O and 12 g into 100 ml of dH_2O, respectively. Then 10% SDS and 10% APS were prepared by dissolving 5 g SDS powder into 50 ml dH_2O and 1 g APS powder into 10 ml dH_2O. The amounts of the reagents that were used to cast gels are given in Table 2.7 and 2.8. Isopropanol was used to prevent any bubble formation between running and stacking gels, then washed off with water after the gel polymerization. 10x SDS-PAGE Running Buffer (recipe given in Table 2.9) was diluted to 1x prior. Equalized protein samples were again heated to 95°C for 5 minutes, vortexed and spun down, then loaded into gels together with protein ladder (ThermoFisher 26619) and ran at 80 V for 30 minutes, followed by 100 V for 1.5-2 hours.

2.4.2 Transfer

In the second part, the PVDF membranes were activated with methanol and Nitrocellulose membranes were activated in ice cold 1x Transfer Buffer (Table 2.11). After the running procedure; the gels were transferred into blotting system, sandwiched between white casette (Anode), sponges, blotting paper, membrane, gel, blotting paper, sponges and black casette (Cathode). The transfer tank was then filled with ice cold 1x Transfer Buffer together with an ice pack in the cold room (+4°C) and ran for 90 minutes at 100 V.

2.4.3 Blocking

Third part begins after the proteins on the gel were transferred to the membranes. For the gels containing Mito samples, Ponceau S staining was performed by washing the nitrocellulose membranes with dye for 5 minutes then visualizing using Biorad-Chemidoc MP imaging system (Bio-Rad, Hercules, CA, USA) in UNAM, Bilkent University. All of the membranes were then washed with TBS-T (Table 2.13) for 10 minutes and blocked at room temperature for 1 hour with 5% Milk or 5% BSA in TBS-T on the shaker.

2.4.4 Primary and Secondary Antibody Incubation

At one hour mark, membranes were again washed with TBS-T for 10 minutes and left at the cold room shaker (+4°C) for 16 hours of primary antibody incubation (Table 2.15). Following 16 hours primary antibody incubation the membranes were washed with TBS-T for 10 minutes, thrice. The membranes were then taken to the room temperature shaker for secondary antibody incubation. Next, the membranes were again washed three times for 10 minutes with changing volumes of TBS-T.

2.4.5 Band Visualization

Amersham ECL prime reagent was used for band detection. Equal volumes of Solution A and Solution B were mixed and warmed up to room temperature. Mixture was then applied to the membranes and visualized using Biorad-Chemidoc MP imaging system in single channel and multichannel modes in the ImageLab software (Biorad, CA, USA).

2.5 RNA isolation

RNA isolation was done by detaching the cells from 6 well plates using 1 ml TriSure (Bioline) reagent. After 200 μl chloroform addition, the eppendorfs were shaken vigorously for 30 seconds and centrifuged for 17 minutes at 15000 rpm at 4°C. Afterwards, the clear part of the mixture (containing RNA) was transferred to another eppendorf containing 500 μl isopropanol, followed by 10 min room temperature incubation, centrifuged again at 15000 rpm for 12 minutes. Pellet was washed with first 75% ethanol and then 99% ethanol with 8000 rpm 8 minutes centrifugation steps in between. Finally, the pellet was dissolved in 20 μl DNase/RNase free water. The measurements were taken in NanoDrop™ 2000.

2.6 cDNA synthesis and q-RT PCR

Complementary Deoxyribonucleic Acid (cDNA) was synthesized from RNA using Revert-aid first strand cDNA Synthesis Kit (Thermo Scientific) according to the company instructions using Bio-Rad C1000 Thermal Cycler. cDNA synthesis steps were as follows; 25°C for 5 minutes, 42°C for 1 hour, 70°C for 5 minutes. After cDNAs have cooled down, they were diluted 1:5 using DNase/RNase free water. The master mix for qPCR includes SYBR green (Roche Light Cycler 480), forward and reverse primers (Table 2.16) and DNase/RNase free water. 8 μl Master Mix was distributed among 96 wells of Bio-Rad Hard-Shell 480 PCR plates together with 2 μl cDNA. SYBR signal coming from each well after each cycle was recorded by Bio-Rad CFX96 Touch Real-Time PCR Detection System. q-RT PCR steps were as follows; first heat 95°C for 15 minutes, then for 45 cycles; 95°C for 10 seconds, 60°C for 30 seconds, 72°C for 30 seconds. SYBR signal coming from each well were obtained after each cycle 96 well Bio-Rad Hard-Shell 480 PCR plates.

2.7 Statistical Analysis

Initially, all populations were tested for normality using Shapiro-Wilk normality test. The data sets that follow Gausian distribution were further analyzed with two tailed t-test with Welch's correction or with Bonferroni corrected One-Way ANOVA, depending on the treatment conditions. For the data sets that do not follow Gausian distribution, Kruskal-Wallis test with Dunn's correction was used. Pearson correlation test was used find whether GFAP and Iba1 correlate in given animal groups. The analyses mentioned above were conducted in Graphpad Prism software (Version 9.1.1) Image J software (NIH, Bethesda, MD, USA) is utilized for Western Blot analysis.

Reagent	Company and Catalog No
β-mercaptoethanol	Applichem A1108,0100
Glycine	Glentham GM2385
Acrylamide 40% solution	Fisher scientific BP1408-1
Bovine Serum Albumin (BSA)	SantaCruz Sc23234
Tris Base	Sigma T1503
Ammonium Persulfate (APS)	Sigma A3678
DC Protein Assay	Biorad 5000116
Chloroform	Sigma-Aldrich 24216
Page Ruler Prestained Protein Ladder	Thermo Fisher Scientific 26619
Triton X	Applichem A 1388,0500
HEPES Buffer	Lonza 17-757F
Protease Inhibitor Cocktail EDTA Free	Sigma P8340-5ML
Phosphatase Inhibitor Cocktail 3	Sigma P0044
Absolute Ethanol	Sigma-Aldrich 32221
PMSF	Ambresco M145-5G
DMEM, high glucose, pyruvate	Gibco 41966029
BSA-Fatty Acid Free	Sigma A7030-500G
Amersham Prime ECL	GE Healthcare RPN2236
DMSO	Sigma 472301
Dulbecco's Phosphate Buffered Saline	Biowest L0625
Penicillin/Streptomycin	Gibco 15140-122
L-glutamine	Sigma G5792
Sodium orthovanadate	Sigma S6508
Roche Light Cycler 480 Sybr green Mix	Roche 4887352001
EDTA	Applichem A3562,1000
PVDF Transfer Membrane	Pierce-Thermo Scientific 88518
Methanol	Sigma-Aldrich 32213
Trisure	Bioline Bio 38033
Palmitate	Sigma P0500

Table 2.2: General Lab Reagents

Sample	dH2O (μl)	BSA(μl)	Concentration (μg/ml)
Blank	5	0	0
Standard 1	4.5	0.5	0.1
Standard 2	4	1	0.2
Standard 3	3	2	0.4
Standard 4	2	3	0.6
Standard 5	1	4	0.8
Standard 6	0	5	1

Table 2.3: Blank and standards preparation for determining protein concentrations with DC Assay

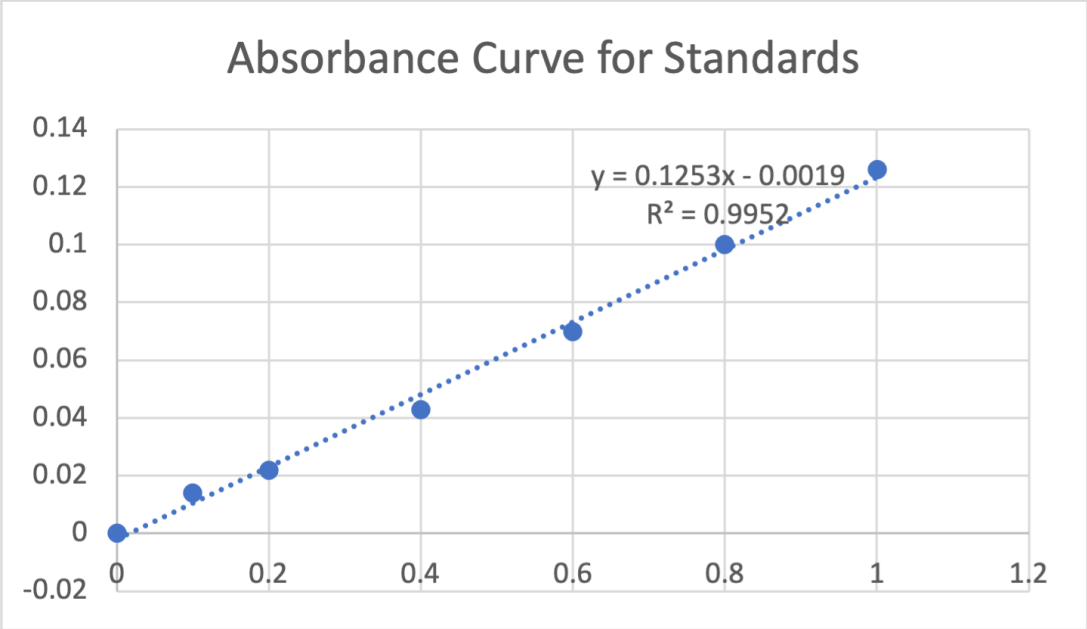

Figure 2.1: Absorbance (OD) curve for protein standards.

1 mM EDTA	400 μl from 0.25 M stock
10 mM HEPES	1000 μl from 1 M stock
250 mM sucrose	8.56 g
Water to	100 ml

Table 2.4: Homogenization Buffer (pH 7.4)

50 mM Tris-HCl pH 7.4	2.5 ml
150 mM NaCl	1.5 ml (0.087 g resolved in 10 ml water)
0.25% (w/v) sodium deoxycholate	0.125 g
1% (v/v) NP-40	0.5 ml
1 mM EDTA	0.1 ml (0.15 g resolved in 500 ml water)

Table 2.5: RIPA Buffer

1000 mM HEPES	5 ml
500 mM EDTA	2 ml
5000 mM NaCl	2 ml
200 mM NaPP	2 ml
500 mM NaF	2 ml
Triton 100X	1 ml
Water	86 ml

Table 2.6: Phospholysis Buffer

Component	10%	12%	15%
Water	3.54 ml	3 ml	2.4 ml
40 % Acrylamide/bis	2.5 ml	3 ml	3.75 ml
1 M Tris-HCl, pH 8.8	3.77 ml	3.75 ml	3.75 ml
10 % SDS	100 μl	100 μl	100 μl
10 % APS	100 μl	100 μl	100 μl
TEMED	10 μl	10 μl	10 μl
Total volume	10 ml	10 ml	10 ml

Table 2.7: Running gel

Component	5%
Water	3.77 ml
40 % Acrylamide/bis	500 μl
1 M Tris-HCl, pH 6.8	625 μl
10 % SDS	50 μl
10 % APS	50 μl
TEMED	5 μl
Total volume	5 ml

Table 2.8: Stacking gel

Tris Base (25 mM)	30 g
Glycine (192 mM)	144 g
SDS (0.1 %)	10 g
Complete with water to	1L

Table 2.9: 10X SDS-PAGE Running buffer

Tris Base (25 mM)	30 g
Glycine (192 mM)	144 g
Complete with water to	1L

Table 2.10: 10X Transfer buffer

10x Transfer Buffer	100 ml
Methanol	200 ml
Complete with water to	1L

Table 2.11: 1X Transfer buffer

Tris-base (100 mM)	24.2 g
NaCl (1500 mM)	80 g
Complete with water to	1L

Table 2.12: 10X TBS (pH 7.6)

10x TBS	100 ml
Water	900 ml
Tween	1 ml

Table 2.13: TBS-T

1M Tris-HCl, pH 6.8 (200mM)	8 ml
Glycerol (40%)	16 ml
SDS (6%)	2.4 g
1 % Bromophenol blue (0.013%)	0.5 ml
Water	12 ml
10% 2-mercaptoethanol	12 ml

Table 2.14: 4x Sample Loading Buffer

Antibody	Company	Catalog No	Condition
PINK1	Thermo Fisher Scientific	710993	1:1000 5% BSA in TBST
SQSTM1/p62	Abcam	ab56416	1:1000 5% BSA in TBST
TOM40	Santa Cruz	D-2/sc-365467	1:1000 5%B SA in TBST
GFAP	Abcam	ab53554	1:2000 5% Milk in TBST
Tubulin	Cell Signaling	2146	1:500 5% Milk in TBST
CHOP	Cell Signaling	5554	1:1000 5% BSA in TBST
Iba1	Abcam	ab178846	1:1000 5% BSA in TBST
Rho GDI	Cell Signaling	2564	1:500 5% BSA in TBST
p-PERK	Cell Signaling	3179S	1:1000 5% BSA in TBST

Table 2.15: Western Blot Antibodies

Gene	Forward	Reverse
LONP1	CTCATGGTGGAGGTTGAGAATG	CAGAGGGTTCAAGGCGATGATA
ATF4	TCGATGCTCTGTTTCGAATG	AGAATGTAAAGGGGGCAACC
CHOP	CCTAGCTTGGCTGACAGAGG	CTGCTCCTTCTCCTTCATGC
PINK1	CCTTCCTATCAGCACCCAAAC	TCCGCTAGTTGAACATACAGGAT
GAPDH	GTGAAGGTCGGTGTGAACG	GGTCGTTGATGGCAACAATCTC

Table 2.16: q-RT PCR primers

Chapter 3

Results

3.1 *In Vivo* Results

In this section, I investigated how the genotype (C57BL/6 and ApoE -/-) and the diet (Chow and Western) affected microglia residing in the cortex of these animals. In order to do that, first I checked the Iba1 (microglial marker) expression with Western Blot analysis. Then, I looked at the correlation between GFAP (astrocyte marker) and Iba1, since astrocytes and microglia are communicating upon any disruption to the homeostasis of the central nervous system such as; neuronal injury, cellular debris and pathogens. So, I wanted to find out if they behave similarly under these stress conditions. To be able to assess correlation, a Pearson correlation test was conducted. All data were reported as mean ±standard error measurement (SEM).

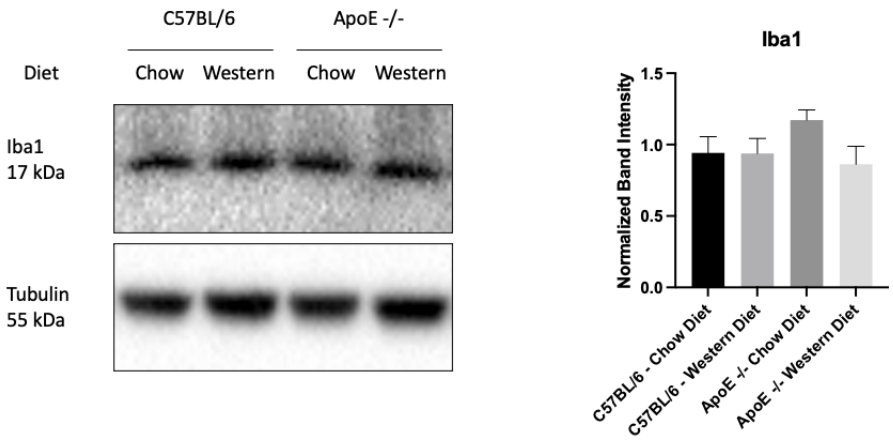

Figure 3.1: Western Blot image of Iba1 (left), and Tubulin normalized Iba1 band intensity among cortex of the C57BL/6 and ApoE -/- Chow and Western Diet groups (right) n=7 for each group.

No signficant effects of genotype (C57BL/6 and ApoE -/-) and diet (chow and western) were observed for Iba1 levels although there were numerical differences. This may be due to the fact that Iba1 exist in both resting and activated microglia forms. Western blot analysis of Iba1 levels does not provide the opportunity to distinguish between the number of active vs resting microglia. Western Blot images were taken by Naz Mengi.

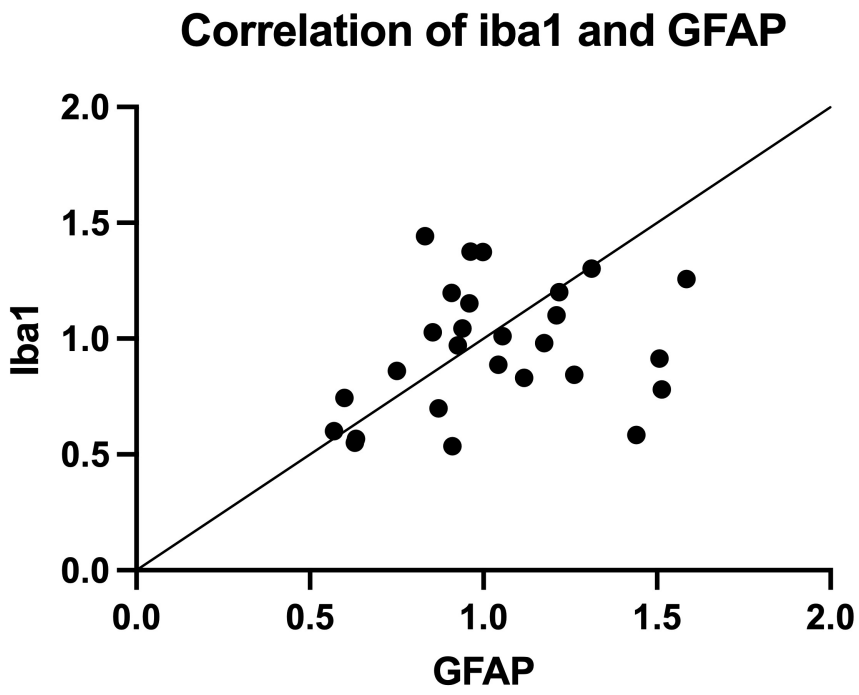

Figure 3.2: Correlation of GFAP (Astrocyte marker) and Iba1 (Microglial marker) for all mice groups (genotype: C57BL/6 and ApoE -/-, diet: Chow and Western). r = 0.2633, p = 0.185.

A Pearson correlation test was conducted in order to observe whether there were any relationship between Iba1 and GFAP levels in the C57BL/6 and ApoE -/- mice brains. A correlation coefficient (r value) was computed as 0.2633, and the p value was 0.185, concluding that there was no correlation between the expression of those two protein levels for all mice. These data suggest that there was no relationship between astroglial and microglial levels. After analyzing relative GFAP protein levels in same animals; Bilge Aşkın found a significant difference between the Western groups of C57BL/6 and ApoE -/- mice (p=0.003) [67]. According to her work, GFAP levels significantly increased in ApoE -/- Western Diet group compared to C57BL/6 Western Diet group. GFAP blots were obtained by Bilge Aşkın, quantification of the data and Pearson analysis was done by me.

Since the brain niche contains many different cell types such as circulating monocytes, granulocytes and dendritic cells [68], I moved the ER stress work into the BV2 cell line model. This would permit me to be able to examine the direct effects of ER stress on microglia.

3.2 *In Vitro* Results

Cell culture experiments were divided in two groups; in the first group I measured two ER stress markers (ATF4 and CHOP) and two mitophagy markers (LONP1 and Pink1) with q-RT PCR using total RNA isolated from BV2 cells (Figures 3.3 and 3.4. Then using Whole Cell Lysates, I checked three ER stress markers (CHOP, p-PERK and p-IRE1 α) with Western Blot analysis (Figures 3.5 3.6 3.7, 3.8, 3.9, 3.10). Then, for the second part, I moved onto isolating mitochondria from those samples. Figures 3.11 and 3.12 show successful mitochondria isolation by looking cytosolic marker Rho GDI and mitochondrial marker TOMM40. Using mitochondria isolated protein samples, I checked two mitophagy markers (p62 and Pink1) with Western Blot. In both parts, Thapsigargin was used to induce ER stress and Palmitate was used to induce mitophagy.

3.2.1 q-RT PCR Results

3.2.1.1 Thapsigargin Treatment

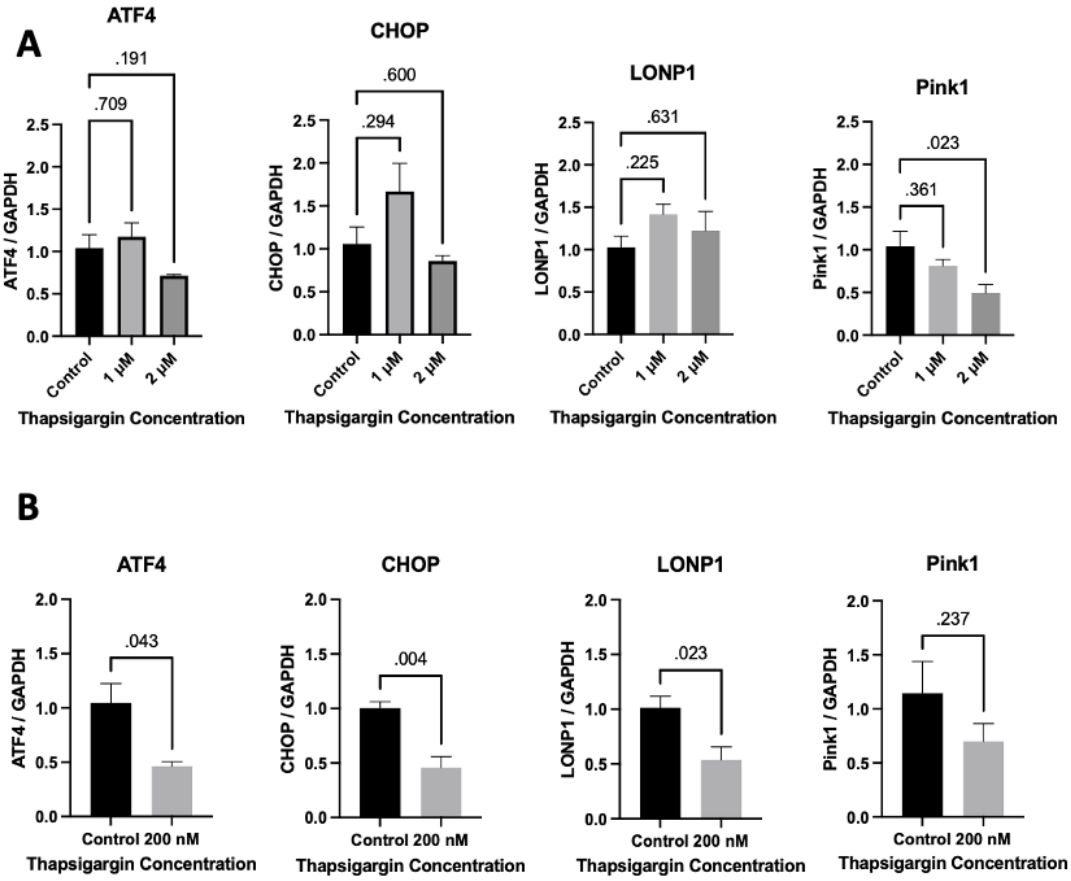

Figure 3.3: q-RT PCR analysis of Thapsigargin Treated BV2 cells from total RNA. A. 1 μM and 2 μM Thapsigargin Treatment for 24 hours (Top), B. 200 nM Thapsigargin Treatment for 24 hours (Bottom).

Initially, the thapsigargin dosage determined as 1 μM and 2 μM for 24 hours from the literature (Figure 3.3A) [65]. However, the high concentration of Thapsigargin killed most of the cells in 24 hours. Thus, no significance was observed for ATF4, CHOP and LONP1. Then, the thapsigargin concentration was reduced to 200 nM for 24 hours, since it has been shown that 200 nM cells still maintain their viability while expressing CHOP (Figure 3.3B) [69]. I started to see significant

differences in ATF4, CHOP and LONP1 levels. Non-significance in Pink1 RNA level could be explained by cluttering of total RNA. Isolating mitochondrial DNA, then assessing Pink1 levels could provide helpful insight on mitophagy levels in the thapsigargin treated cells.

3.2.1.2 Palmitate Treatment

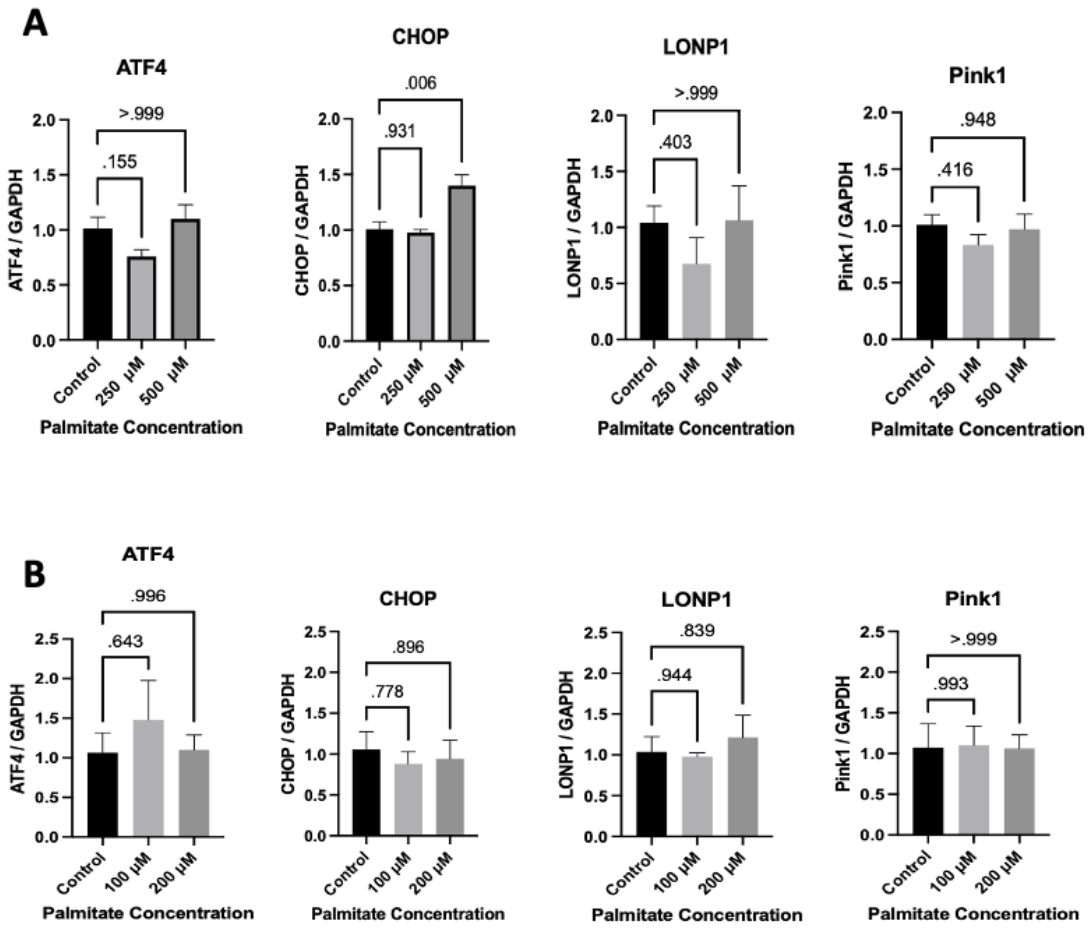

Figure 3.4: q-RT PCR analysis of Palmitate Treated BV2 cells from total RNA A. 250 μM and 500 μM Palmitate Treatment for 16 hours (Top), B. 100 μM and 200 μM Palmitate Treatment for 24 hours (Bottom).

First, I tried to induce mitophagy by treating BV2 cells with palmitate for 16 hours, with concentrations 250 μM and 500 μM (Figure 3.4A), however the duration and dosages were not enough to induce ER stress or mitophagy. In part B, treatment duration was elongated to 24 hours, but the Palmitate dosage was reduced to 100 μM and 200 μM based on a study in BV2 cells [66]. Unfortunately, the results of that study could not be replicated here. No significant difference has been observed for ATF4, CHOP, LONP1 and Pink1 at RNA levels. A potential problem could be the palmitate aggregation, which doesn't enter the cells to extort its effects equally, thus causing no significant changes.

3.2.2 Whole Cell Lysate Western Blots

3.2.2.1 Thapsigargin Treatment

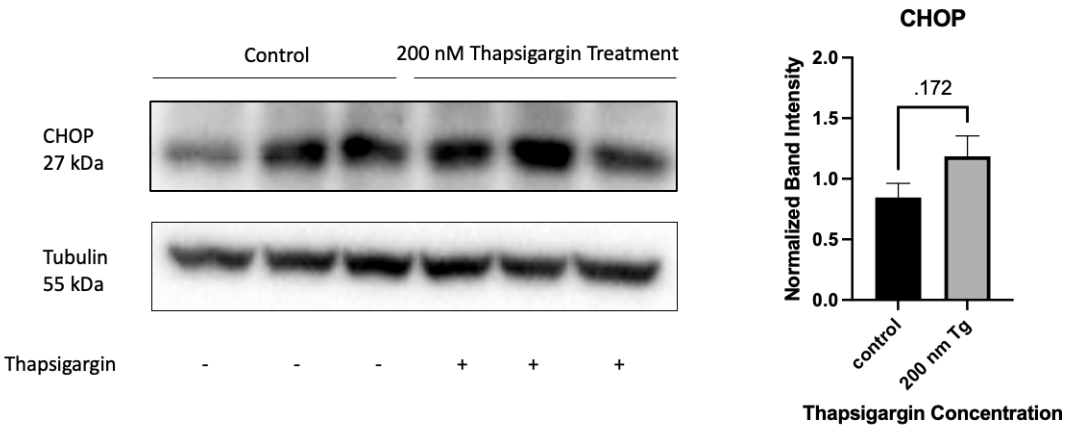

Figure 3.5: Western Blot Analysis of CHOP in 24 hours 200 nM Thapsigargin Treated BV2 cells. Representative Western Blot image (left), quantification using t-test (right), p=0.172.

Although the difference was not significant (p=0.172), CHOP protein levels seem to be increasing with Thapsigargin treatment, which was consistent with the notion that Thapsigargin increases ER stress.

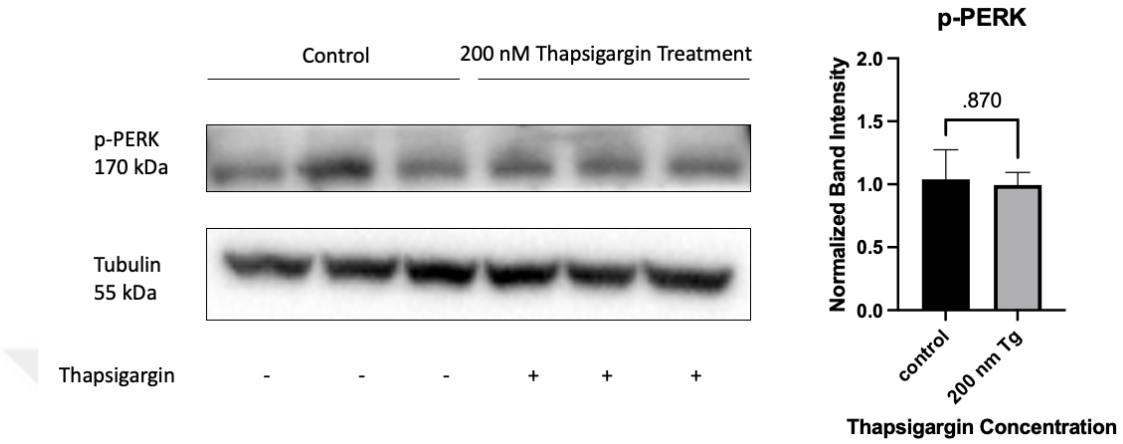

Figure 3.6: Western Blot Analysis of p-PERK in 24 hours 200 nM Thapsigargin Treated BV2 cells. Representative Western Blot image (left), quantification using t-test (right), p=0.87.

No significant difference was observed for p-PERK levels in thapsigargin treated cells (p=0.87). As discussed in the next chapter, 24 hours of treatment could prevent measuring any changes in the phosphorylation levels.

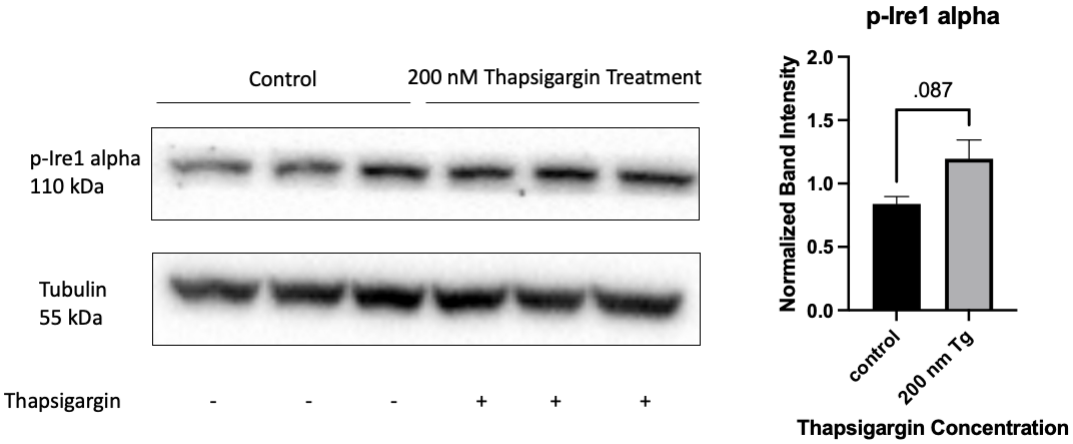

Figure 3.7: Western Blot Analysis of p-IRE1 αin 24 hours 200 nM Thapsigargin Treated BV2 cells. Representative Western Blot image (left), quantification using t-test (right), p=0.087.

p-IRE1 αprotein level was marginally significant (p=0.087) between thapsigargin treated and non-treated cells, showing a slight increase due to the treatment. It shows ER stress activation might be by IRE1 pathway instead of PERK pathway.

3.2.2.2 Palmitate Treatment

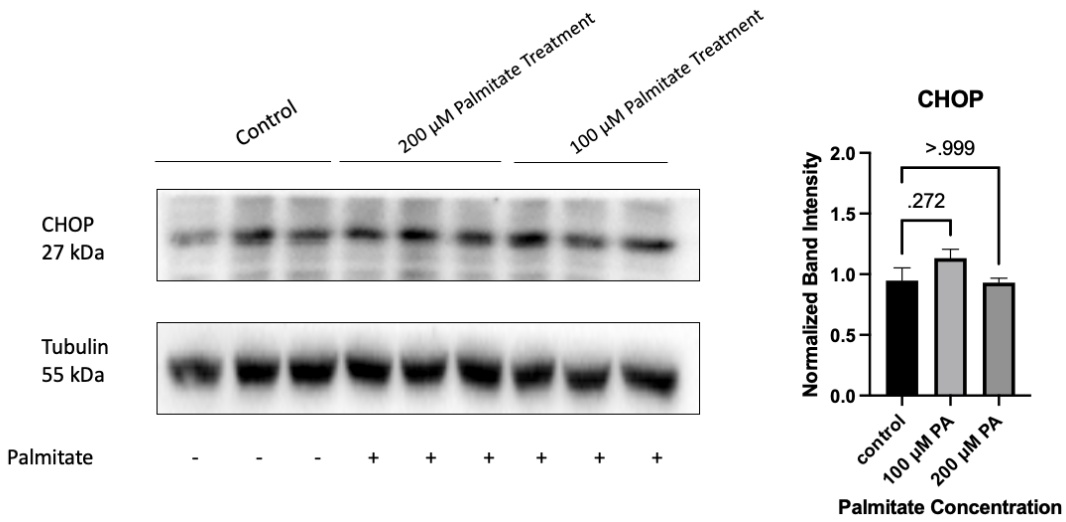

Figure 3.8: Western Blot Analysis of CHOP in 24 hours 100 μM and 200 μM Palmitate Treated BV2 cells. Representative Western Blot image (left), quantification using one-way ANOVA (right), p=0.272 for 100 μM Palmitate.

There was a slight increase of CHOP in 100 μM Palmitate treated samples compared to control, and almost no difference to 200 μM, suggesting that the optimal dosage to induce CHOP could be less than/around 100 μM. The inverted U-shaped dose-effect observed with the CHOP protein levels. It is a phenomenon, when increasing the dosage of a compound, reagent or drug increases the effect to a maximum and then effect decreases [70].

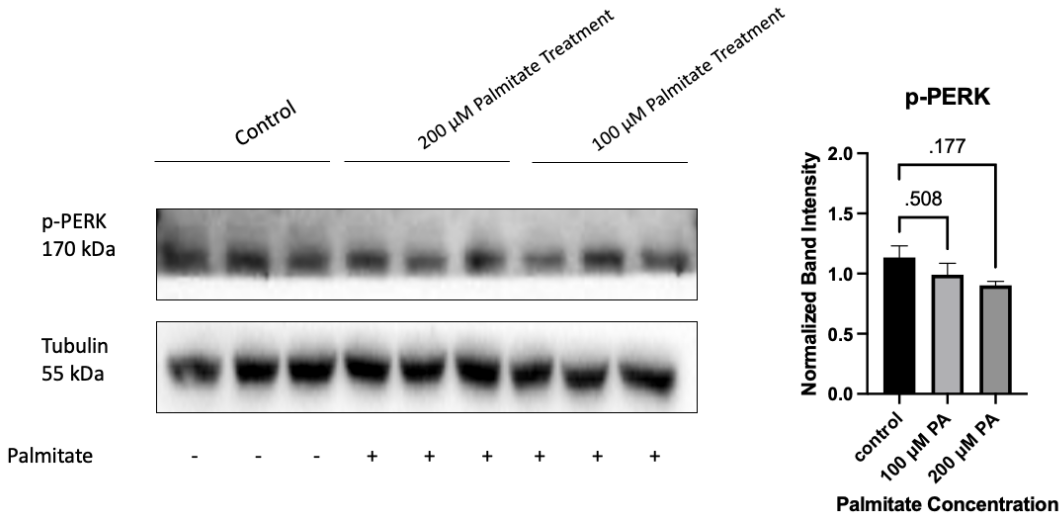

Figure 3.9: Western Blot Analysis of p-PERK in 24 hours 100 μM and 200 μM Palmitate Treated BV2 cells. Representative Western Blot image (left), quantification using one-way ANOVA (right), p=0.508 for 100 μM and p=0.177 for 200 μM Palmitate.

Similar to thapsigargin results, p-PERK did not significantly differ between groups. It was easy to miss critical time period for phosphorylation in 24 hours. In the future, this experiment could be repeated by taking samples at 3, 6, 9, 12 and 18 hours into the treatment and incubating them with p-PERK and total PERK antibodies to determine the optimal treatment time.

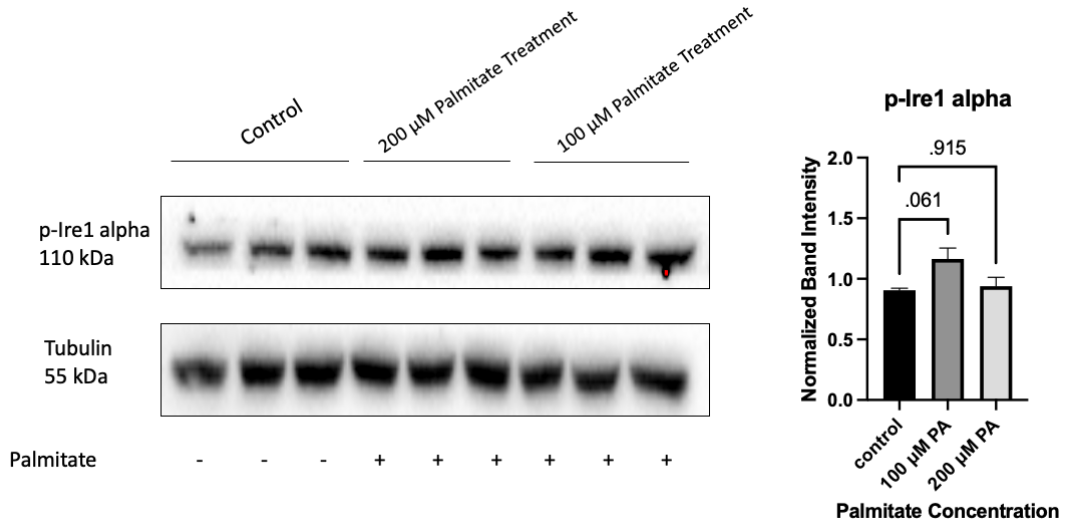

Figure 3.10: Western Blot Analysis of p-Ire1 αin 24 hours 100 μM and 200 μM Palmitate Treated BV2 cells. Representative Western Blot image (left), quantification using one-way ANOVA (right), p=0.061 for 100 μM and p=0.915 for 200 μM Palmitate.

Coinciding with the thapsigargin treatment, p-IRE1 $\alpha$was marginally significant (p=0.061) between control and 100 μM Palmitate treated samples, once again suggesting that ER stress might be carried with IRE1 pathway in microglia. Still, this result was not conclusive without looking further into the IRE1 pathway markers.

3.2.3 Mitochondria Isolation

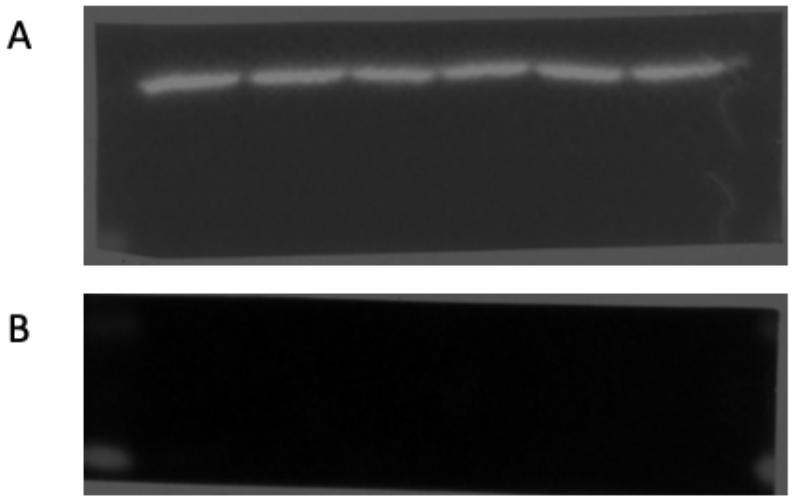

Figure 3.11: Cytosolic (top) and Mitochondrial (bottom) blots showing Rho GDI expression.

The cytosolic (A) and mitochondrial proteins (B) were incubated with Rho GDI antibody and visualized in Biorad-Chemidoc MP imaging system. Due to Rho GDI being a cytosolic marker, having no expression in mitochondrial proteins when filmed together with cytosolic proteins proves that mitochondrial isolation in BV2 cells was working.

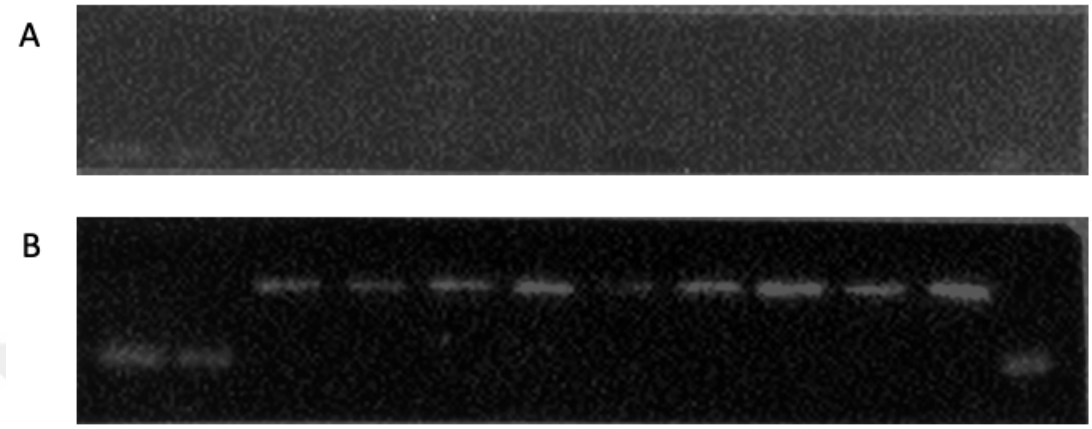

Figure 3.12: Cytosolic (top) and Mitochondrial (bottom) blots showing TOMM40 expression.

As a second BV2 mitochondrial isolation control, cytosolic (A) and mitochondrial proteins (B) were incubated with TOMM40 (Translocase Of Outer Mitochondrial Membrane 40) antibody and visualized together. Due to TOMM40 being a mitochondrial protein, its expression was greater in mitochondrial proteins (bottom) compared to cytosolic proteins (top) when exposed for the same amount of time in Biorad-Chemidoc MP imaging system.

3.2.4 Mitochondrial Extract Western Blots

Mitochondria were isolated from thapsigargin and palmitate treated BV2 cells, in order to have a better understanding of what was going inside the mitochondria. Mitochondrial extract blots were normalized to Ponceau S staining.

3.2.4.1 Thapsigargin Treatment

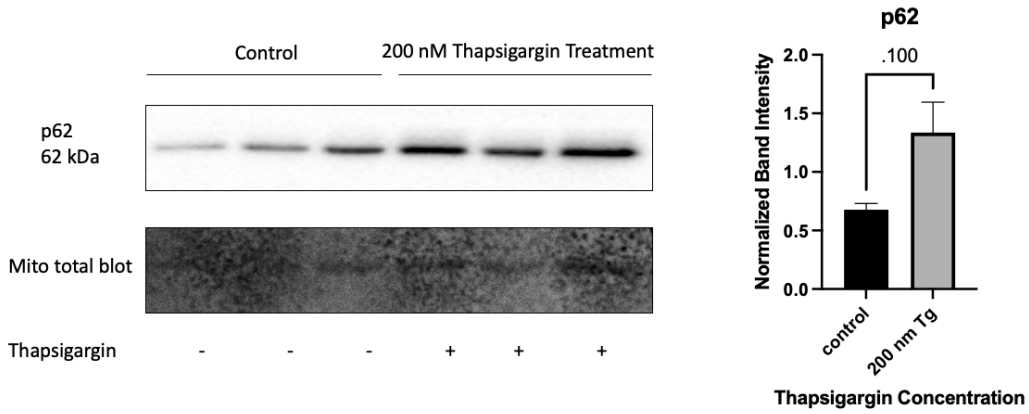

Figure 3.13: Western Blot Analysis of p62 in 24 hours 200 nM Thapsigargin Treated BV2 cells. Representative Western Blot image (left), quantification using t-test (right), p=0.1.

p62/SQSTM1 protein level was marginally increasing with thapsigargin treatment (p=0.1). p62 is an adaptor protein of mitophagy and it facilitates engulfment of the dysfunctional mitochondria by autophagosomes to be digested. Therefore increase in p62 levels show the initial sign of mitophagy in these samples. Taken together with increase in ER stress markers, it is possible to assume that mitochondria were also affected from thapsigargin treatment.

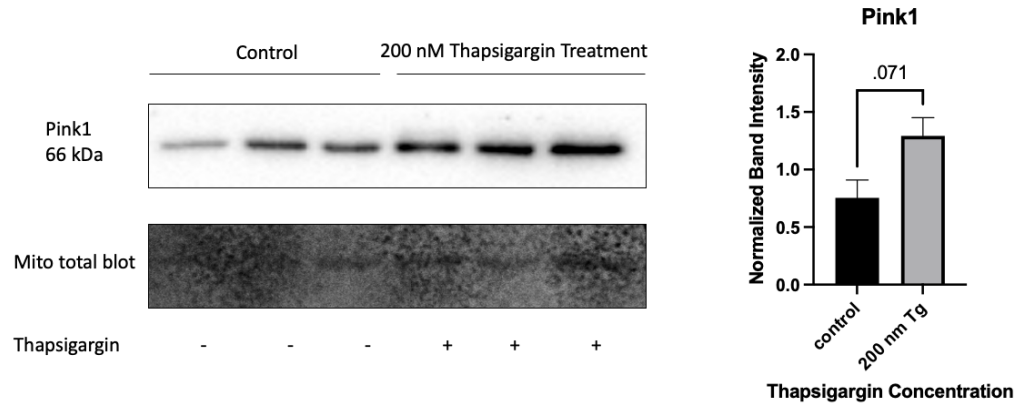

Figure 3.14: Western Blot Analysis of Pink1 in 24 hours 200 nM Thapsigargin Treated BV2 cells. Representative Western Blot image (left), quantification using t-test (right), p=0.071.

Pink1 is the main mitophagy marker. It acts as a distress signal by phosphorylating Parkin to initiate further mitophagy cascade with the help of p62. The fact that they were both increasing with thapsigargin further proves that thapsigargin induces mitochondrial autophagy in this microglial cell line.

3.2.4.2 Palmitate Treatment

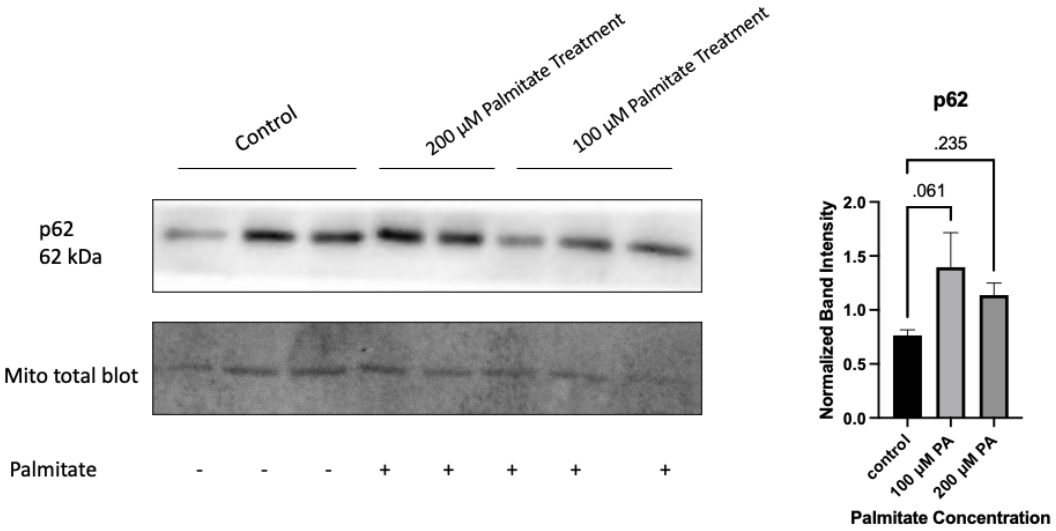

Figure 3.15: Western Blot Analysis of p62 in 24 hours 100 μM and 200 μM Palmitate Treated BV2 cells. Representative Western Blot image (left), quantification using Kruskal Wallis test (right), p=0.061 for 100 μM and p=0.235 for 200 μM Palmitate.

p62 increase was almost significant (p=0.061) between control and 100 μM palmitate treated samples, suggesting that 100 μM was a better dosage than 200 μM to induce mitophagy in BV2 cells. p62 levels increase under mitochondrial stress conditions, when the mitochondria were undergoing phagocytosis by lysosomes in the structures called autophagosomes. The results coincide with the thapsigargin treatment.

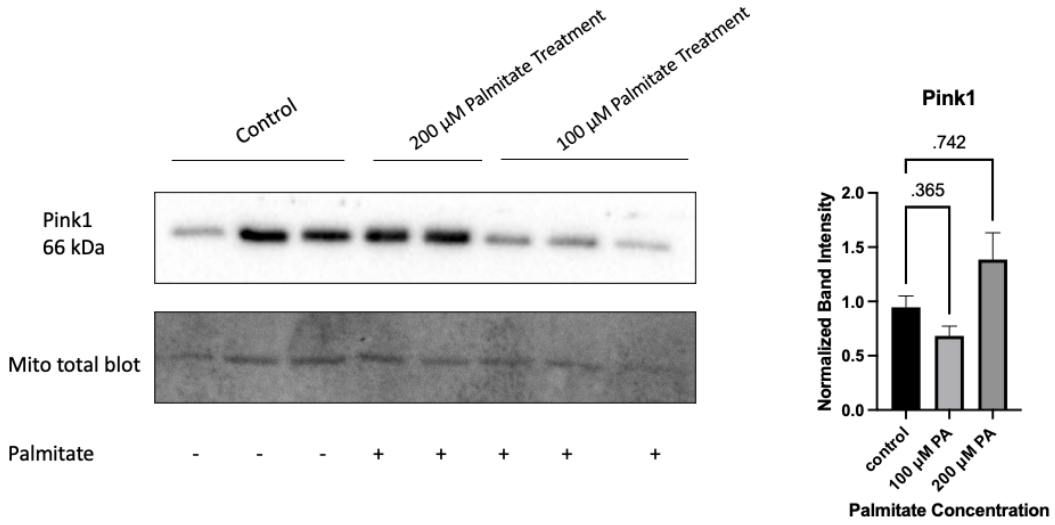

Figure 3.16: Western Blot Analysis of Pink1 in 24 hours 100 μM and 200 μM Palmitate Treated BV2 cells. Representative Western Blot image (left), quantification using Kruskal Wallis test (right), p=0.365 for 100 μM and p=0.742 for 200 μM Palmitate.

In this figure, Pink1 did not follow the same pattern as previously. An increase was observed with 200 μM of palmitate treatment, whereas 100 μM caused a decrease in Pink1 levels. Mitochondria are dynamic organelles, their turnover rate (biogenesis/mitophagy) is rather rapid, with half-life around 3 days for the mouse liver and 14 for heart [71]. Thus, as discussed for p-PERK levels, 24 hours of palmitate treatment may not be optimal duration to observe full blown mitophagy response in these cells.

Chapter 4

Discussion and Future Work

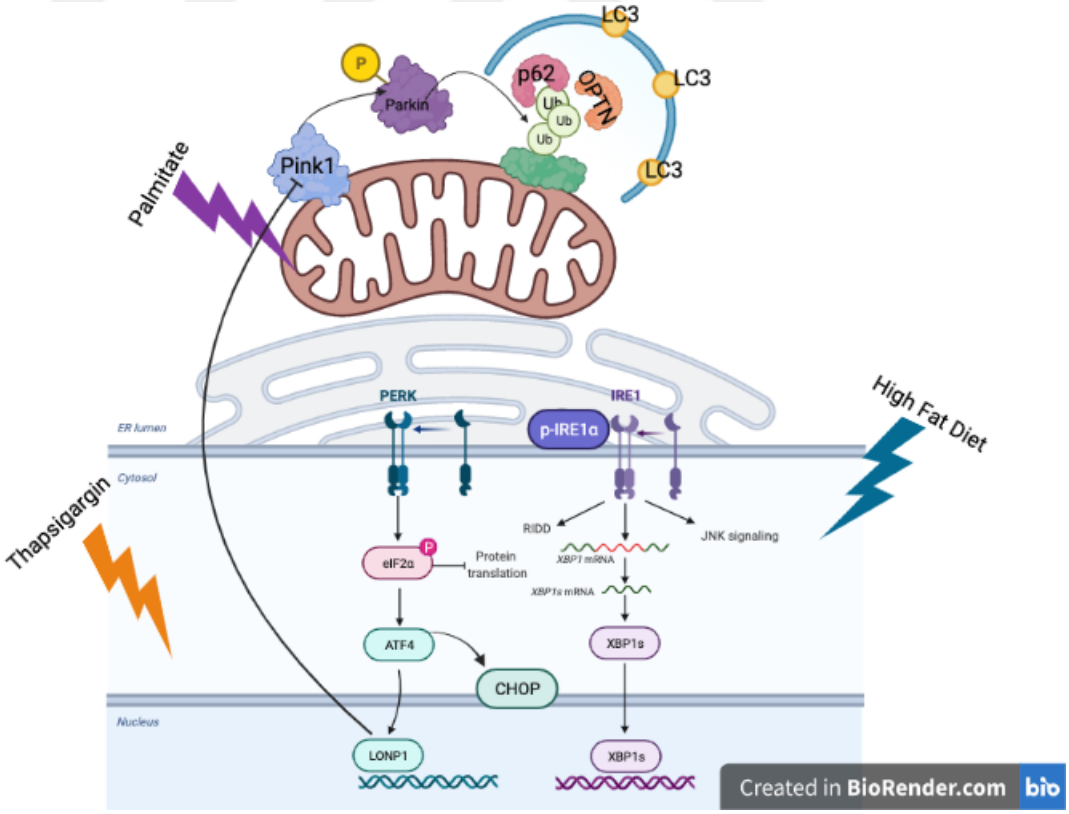

Figure 4.1: Summary figure showing the induced organelle stress with factors such as high-fat diet, thapsigargin and palmitate in ER and mitochondria. This image is created with BioRender.com.

Figure 4.1 summarizes the experiments conducted in this thesis to offer a broad understanding of the processes going on in the microglial cells. So far, I showed that 200 nM thapsigargin treatment for 24 hours induces ER stress by increasing CHOP and p-IRE1 αprotein levels. Decrease in ATF4 and CHOP mRNA levels could be explained by the PERK auto-regulation, meaning that if the source of stress is not removed after induction of UPR, CHOP induces eIF2 αdephosphorylation, thus promoting apoptosis. Cells undergoing apoptosis normally decreases transcription of non-apoptotic genes. 24 hour 100 μM Palmitate treatment also marginally increased CHOP protein levels (p=0.061). In addition to these results, I showed that the pure mitochondria can be isolated from BV2 cells by centrifugation. Using these mitochondrial extracts, I assessed mitophagy with Pink1 and p62 antibodies. p62 levels have increased with both treatments (p=0.061 for 100 μM palmitate and p=0.1 for thapsigargin). Pink1 was also marginally significant with thapsigargin treatment (p=0.071), but it was not the case for palmitate treatment, and the reasons are explained below. Overall, ER stress activation by thapsigargin treatment increases mitophagy in BV2 mouse microglial cell line.

An increase in ER stress markers such as CHOP and p-IRE1 αhas been observed with both treatments. While CHOP protein levels could not reach significance, there was an increasing numerical trend. p-IRE1 $\alpha$was marginally significant for both treatments (p=0.087 for thapsigargin and p=0.061 for 100 μM palmitate). Mitophagy indicators (Pink1 and p62) were assessed with Western Blot analysis after successful mitochondria isolation from BV2 cells. The data indicated that p62 marginally increased with both palmitate (p=0.61) and thapsigargin (p=0.1) treatments. Following both treatments, very subtle effects of ER stress were observed. This suggests that further experiments examining optimal dosage and duration need to be performed. Overall, the induction of ER stress appears to induce mitophagy and alter microglia, which likely leads to altered cellular and synaptic function.

In Figure 3.1, genotype and diet did not influence microglial marker Iba1. This could be the case because of couple reasons; firstly, (as discussed earlier) the central nervous system is not only composed of microglial cells but many others, thus clouding the microglial expression. Which is why we decided to include *in*

vitro part to have pure microglial results. Iba1 is not a marker to distinguish active and resting states of microglia, FACS method is. Also, there was no correlation between Iba1 and GFAP levels. This could be due to antibodies not reflecting actual number of those cells but simply the expression. The only way to prove that the microglia and astrocyte cell numbers are equal would be by conducting Immunohistochemistry (IHC) analysis. It is possible that, we are facing ceiling effect when it comes to ApoE -/- mice with maximum Iba1 expression.

In Vitro part showed that published cell line results are not always replicable, due to cell culture being susceptible to many changes such as medium ingredients, method of palmitate preparation, passage number of the cells (accumulation of mutations), and method of immortalization (J2 virus in this case). Palmitate ($C_{16}H_{32}O_2$) has an amphipathic structure, containing both hydropobic and hydrophilic parts [72]. Due to its water insoluble nature and melting at 60°C, it was prepared in ethanol and added to 65°C 1% fatty acid free BSA complex in DMEM. However, it possible that it formed aggregates within this complex and couldn't penetrate the cells homogeneously. A study concluded that while 1% ethanol was too toxic to the cells, 0.1% ethanol was not enough dissolve hydrophobic reagents [73]. In this thesis, ratio of palmitate dissolved in ethanol to the total medium was 0.1% based on previous published work to prevent any cytotoxicity [15]. This may be the reason for non-significant RNA levels with palmitate treatment.

p-PERK protein levels did not significantly differ with thapsigargin or palmitate treatments, a possible explanation is phosphorylation being a transient event and 24 hours treatment could have missed the peak periods when phosphorylation occurs. While p-PERK did not change drastically, p-IRE1 αprotein levels were marginally significant in this cell line, suggesting that ER stress may be carried with IRE1 pathway in microglia. Even though, further research with in-depth analysis of IRE1 pathway markers are required to conclude this was the case, it is logical to assume with increase in ER stress mitochondrial stress increases, inducing mitophagy response. Aligned with this reasoning, p62 and Pink1 marginally increased with 200 nM Thapsigargin treatment, showing mitophagy was taking place with treatment. This was consistent with decreasing LONP1 RNA levels,

since LONP1 degrades Pink1 to block mitophagy cascade initiation.

A drawback was not being able to infer protein levels for CHOP and Pink1 from RNA levels. Checking those markers in mitochondrial DNA (mtDNA) isolated samples could provide insight on mitophagy mechanism. Investigating mtDNA levels could also help speculating the number of mitochondria in these cells. Moreover, the differences in protein levels could be due to a feedback mechanism. As explained in the first chapter, activation of PERK pathway starts when PERK phosphorylates serine 51 on eIF2 $\alpha$to stop global protein translation. CHOP is activated to initiate apoptosis as a last resort for the stressed ER. Marciniak et al., showed that CHOP initiates apoptosis by activating growth arrest and DNA damage-34 (GADD34), which dephosphorylates eIF2 αtogether with phosphatase 1 protein (PP1) under stress conditions [74]. This dephosphorylation rescues restrained translation, but also causes apoptotic genes to be translated as well. If the cell was undergoing apoptosis, then it makes sense for non-apoptotic mRNA levels to be decreasing. So, CHOP's interference could reverse the effects of PERK pathway, which could explain the counter intuitive results showing induced mitophagy with activated PERK.

Also, mitochondria turnover (biogenesis/autophagy) is a dynamic intracellular process, so it may not be always possible to catch mitochondria undergoing mitophagy. So, for this study, timing of the treatments could be off, even though treatment dosages and duration was based in published articles [65], [66] and [69]. For example, I observed 24 hours 1 μM and 2 μM thapsigargin treatment caused significant cell death in BV2 cells, contradictory to the work of Piers and colleagues [65]. Also, Nakandakari et al., showed that with longer exposure of palmitate on BV2 cells (10 days) inflammatory and apoptotic genes were expressed in higher amounts in this cell line [75]. So, for the future work, in order to determine the optimal dosage and duration of these treatments, cell death could be assessed using MTT Assay and Cell Titer Glo [76]. Another parameter to asses mitochondrial health could be the Oxygen Consumption Rate (OCR), which was measured by Seahorse Assay described here [77].

Decrease in number of mitochondria by to mitophagy could be detrimental to the brain cells if there is not enough mitochondrial biogenesis to balance the energy demand. Mitochondrial biogenesis is regulated through the Peroxisome proliferator-activated receptor gamma, co-activator 1 alpha (PGC-1 α)/ATF6 αComplex [78]. Most of the brain mitochondrial biogenesis studies were conducted in the context of sports and physical exercise, as opposite to animals in hyperlipidemic or obese states [79]. So, the evaluation of PGC-1 αlevels in ApoE -/- mice and in BV2 cells could provide a deeper understanding about mitochondrial turnover rates under stress conditions.

Figures 3.11 and 3.12 show that mitochondria can be isolated from BV2 cells using method described in Section 2.2.3 Mitochondria Isolation. This was the first successful mitochondria isolation in the BV2 mouse microglial cell line. By utilizing the same procedure for tissues, mitochondria could be isolated from same animals (C57BL/6 and ApoE -/-) in the future. Mitochondria isolation from brains could provide insight to how high fat diet and genetics contribute to mitophagy in mouse brains. Also morphological changes in mitochondria could be observed using confocal microscopy upon thapsigargin and palmitate stress, with the methods described in this article [80]. Again using same animals, microglia isolation or establishing primary microglial culture could shed light on the differences between *in vivo* and *in vitro* systems for ER stress and mitophagy. Primary microglia could even be co-cultured with astroglial cells to study the effects of palmitate. Furthermore, investigation of Iba1 levels in hippocampus of C57BL/6 and ApoE -/- mice, (since hippocampus is vulnerable to the changes in inflammation caused by constant fatty acid intake) could provide insight into how microglia were affected from high fat diet in different regions [81].

A rising issue in science community is the lack of female mice data. Female mice were disregarded since many researchers believed that their estrous cycle would add further variability and complicate their study by increasing the mice numbers [82]. However, it has been proven that the variations in female mice are not greater than males [83]. This doesn't mean that females aren't worthy to study, since males and females have different responses to internal and external stimuli [84]. There are studies which look at ER stress and mitophagy in female

mice; one such group investigated whether gender plays a role in kidney function under ER stress, and found that females have higher tolerance to tunicamycin (ER stressor like thapsigargin) and less apoptotic response compared to males [85]. On the contrary, young female mice showed higher levels of autophagy and mitophagy proteins with mitochondrial stress [86]. Even though BV2 cells were originated from female mice, *in vivo* part of this thesis was only experimented on male mice. This was another limitation of this study. In the future, it is worth to investigate how ER stress affects microglia in the brains of female mice.

To conclude, these data show that ER stress induces mitophagy and it results in alteration of microglia. Consistent with the literature, thapsigargin and palmitate induced ER stress proteins and promoted mitophagy in the microglial cells. Unexpectedly, while the ER stress protein levels increased with thapsigargin treatment, mRNA levels showed a decreasing trend. This is explained by PERK pathway auto-regulation, where CHOP induces apoptotic pathways under extreme stress conditions. Also, it has been shown in the literature that palmitate increases mRNA levels of ER stress markers, however no significance was observed in this setting. Further analysis will be needed to determine the optimal timing and dosages for ER stress induction in order to provide a model for examining the deleterious effects of lipid-induced organelle stress.

Bibliography

[1] R. T. Hurt, C. Kulisek, L. A. Buchanan, and S. A. McClave, "The obesity epidemic: challenges, health initiatives, and implications for gastroenterologists," *Gastroenterol Hepatol (N Y)*, vol. 6, pp. 780–792, Dec 2010.

[2] R. N. Bergman and M. Ader, "Free fatty acids and pathogenesis of type 2 diabetes mellitus," *Trends Endocrinol Metab*, vol. 11, pp. 351–356, Nov 2000.

[3] I. T. de Almeida, H. Cortez-Pinto, G. Fidalgo, D. Rodrigues, and M. E. Camilo, "Plasma total and free fatty acids composition in human non-alcoholic steatohepatitis," *Clin Nutr*, vol. 21, pp. 219–223, Jun 2002.

[4] Y. Duan, L. Zeng, C. Zheng, B. Song, F. Li, X. Kong, and K. Xu, "Inflammatory links between high fat diets and diseases," *Frontiers in Immunology*, vol. 9, 2018.

[5] J. Lu, D.-m. Wu, Z.-h. Zheng, Y.-l. Zheng, B. Hu, and Z.-f. Zhang, "Troxerutin protects against high cholesterol-induced cognitive deficits in mice," *Brain*, vol. 134, pp. 783–797, 01 2011.

[6] F. Binayi, M. Moslemi, F. Khodagholi, M. Hedayati, and H. Zardooz, "Long-term high-fat diet disrupts lipid metabolism and causes inflammation in adult male rats: possible intervention of endoplasmic reticulum stress," *Archives of Physiology and Biochemistry*, vol. 0, no. 0, pp. 1–9, 2020. PMID: 32907408.

[7] L. Tan, L. Harper, M. A. McNulty, C. S. Carlson, and R. R. Yammani, "High-fat diet induces endoplasmic reticulum stress to promote chondrocyte apoptosis in mouse knee joints," *FASEB J*, vol. 34, pp. 5818–5826, 04 2020.

[8] M. R. Lee, S. J. Bae, J. E. Kim, B. R. Song, J. Y. Choi, J. J. Park, J. W. Park, M. J. Kang, H. J. Choi, Y. W. Choi, K. M. Kim, and D. Y. Hwang, "," *Lab Anim Res*, vol. 34, pp. 288–294, Dec 2018.

[9] L. K. Townsend, K. D. Medak, W. T. Peppler, G. M. Meers, R. S. Rector, P. J. LeBlanc, and D. C. Wright, "High-saturated-fat diet-induced obesity causes hepatic interleukin-6 resistance via endoplasmic reticulum stress[s]," *Journal of Lipid Research*, vol. 60, no. 7, pp. 1236–1249, 2019.

[10] Y. Chen, Z. Wu, S. Zhao, and R. Xiang, "Chemical chaperones reduce er stress and adipose tissue inflammation in high fat diet-induced mouse model of obesity," *Scientific Reports*, vol. 6, p. 27486, Jun 2016.

[11] J. Poirier, "Apolipoprotein e in animal models of cns injury and in alzheimer's disease," *Trends in Neurosciences*, vol. 17, no. 12, pp. 525–530, 1994.

[12] Y. Huang and R. W. Mahley, "Apolipoprotein E: structure and function in lipid metabolism, neurobiology, and Alzheimer's diseases," *Neurobiol Dis*, vol. 72 Pt A, pp. 3–12, Dec 2014.

[13] S. H. Zhang, R. L. Reddick, J. A. Piedrahita, and N. Maeda, "Spontaneous hypercholesterolemia and arterial lesions in mice lacking apolipoprotein E," *Science*, vol. 258, pp. 468–471, Oct 1992.

[14] E. McNeill, K. M. Channon, and D. R. Greaves, "Inflammatory cell recruitment in cardiovascular disease: murine models and potential clinical applications," *Clinical Science*, vol. 118, pp. 641–655, 03 2010.

[15] U. I. Onat, A. D. Yildirim, Özlem Tufanli, I. Çimen, B. Kocatürk, Z. Veli, S. M. Hamid, K. Shimada, S. Chen, J. Sin, P. K. Shah, R. A. Gottlieb, M. Arditi, and E. Erbay, "Intercepting the lipid-induced integrated stress response reduces atherosclerosis," *Journal of the American College of Cardiology*, vol. 73, no. 10, pp. 1149–1169, 2019.

[16] L. Lawson, V. Perry, P. Dri, and S. Gordon, "Heterogeneity in the distribution and morphology of microglia in the normal adult mouse brain," *Neuroscience*, vol. 39, no. 1, pp. 151–170, 1990.

[17] M. Greter, I. Lelios, and A. L. Croxford, "Microglia versus myeloid cell nomenclature during brain inflammation," *Frontiers in Immunology*, vol. 6, 2015.

[18] I. V. Milanova, M. J. T. Kalsbeek, X.-L. Wang, N. L. Korpel, D. J. Stenvers, S. E. C. Wolff, P. de Goede, A. C. Heijboer, E. Fliers, S. E. la Fleur, A. Kalsbeek, and C.-X. Yi, "Diet-induced obesity disturbs microglial immunometabolism in a time-of-day manner," *Frontiers in Endocrinology*, vol. 10, 2019.

[19] S. Voet, M. Prinz, and G. van Loo, "Microglia in central nervous system inflammation and multiple sclerosis pathology," *Trends in Molecular Medicine*, vol. 25, pp. 112–123, Feb 2019.

[20] K. Ohsawa, Y. Imai, Y. Sasaki, and S. Kohsaka, "Microglia/macrophage-specific protein iba1 binds to fimbrin and enhances its actin-bundling activity," *Journal of Neurochemistry*, vol. 88, no. 4, pp. 844–856, 2004.

[21] K. E. Hopperton, D. Mohammad, M. O. Trépanier, V. Giuliano, and R. P. Bazinet, "Markers of microglia in post-mortem brain samples from patients with alzheimer's disease: a systematic review," *Molecular Psychiatry*, vol. 23, pp. 177–198, Feb 2018.

[22] E. M. Hol and M. Pekny, "Glial fibrillary acidic protein (GFAP) and the astrocyte intermediate filament system in diseases of the central nervous system," *Curr Opin Cell Biol*, vol. 32, pp. 121–130, Feb 2015.

[23] H. Wang, J. A. Kulas, C. Wang, D. M. Holtzman, H. A. Ferris, and S. B. Hansen, "Regulation of beta-amyloid production in neurons by astrocyte-derived cholesterol," *Proceedings of the National Academy of Sciences*, vol. 118, no. 33, 2021.

[24] E. Blasi, R. Barluzzi, V. Bocchini, R. Mazzolla, and F. Bistoni, "Immortalization of murine microglial cells by a v-raf / v-myc carrying retrovirus," *Journal of Neuroimmunology*, vol. 27, pp. 229–237, May 1990.

[25] B. Stansley, J. Post, and K. Hensley, "A comparative review of cell culture systems for the study of microglial biology in alzheimer's disease," *Journal of Neuroinflammation*, vol. 9, p. 115, May 2012.

[26] B. K. Atwood, J. Lopez, J. Wager-Miller, K. Mackie, and A. Straiker, "Expression of g protein-coupled receptors and related proteins in hek293, att20, bv2, and n18 cell lines as revealed by microarray analysis," *BMC Genomics*, vol. 12, p. 14, Jan 2011.

[27] A. Henn, S. Lund, M. Hedtjärn, A. Schrattenholz, P. Pörzgen, and M. Leist, "The suitability of BV2 cells as alternative model system for primary microglia cultures or for animal experiments examining brain inflammation," *ALTEX*, vol. 26, no. 2, pp. 83–94, 2009.

[28] D. S. Schwarz and M. D. Blower, "The endoplasmic reticulum: structure, function and response to cellular signaling," *Cellular and Molecular Life Sciences*, vol. 73, pp. 79 – 94, 2015.

[29] I. Braakman and D. N. Hebert, "Protein folding in the endoplasmic reticulum," *Cold Spring Harb Perspect Biol*, vol. 5, p. a013201, May 2013.

[30] C. Hetz, "The unfolded protein response: controlling cell fate decisions under er stress and beyond," *Nature Reviews Molecular Cell Biology*, vol. 13, pp. 89–102, Feb 2012.

[31] D. Ron and P. Walter, "Signal integration in the endoplasmic reticulum unfolded protein response," *Nature Reviews Molecular Cell Biology*, vol. 8, pp. 519–529, Jul 2007.

[32] H. P. Harding, Y. Zhang, A. Bertolotti, H. Zeng, and D. Ron, "Perk is essential for translational regulation and cell survival during the unfolded protein response," *Molecular Cell*, vol. 5, no. 5, pp. 897–904, 2000.

[33] R. Akai, A. Hosoda, M. Yoshino, and T. Iwawaki, "Constitutive role of gadd34 and crep in cancellation of phospho-eif2 -dependent translational attenuation and insulin biosynthesis in pancreatic cells," *Genes to Cells*, vol. 20, no. 11, pp. 871–886, 2015.

[34] K. Szczepanowska and A. Trifunovic, "Mitochondrial matrix proteases: quality control and beyond," *FEBS J*, May 2021.

[35] T. B. Rogers, G. Inesi, R. Wade, and W. J. Lederer, "Use of thapsigargin to study Ca2+ homeostasis in cardiac cells," *Bioscience Reports*, vol. 15, pp. 341–349, 10 1995.

[36] R. Bertram, M. Gram Pedersen, D. S. Luciani, and A. Sherman, "A simplified model for mitochondrial atp production," *Journal of Theoretical Biology*, vol. 243, no. 4, pp. 575–586, 2006.

[37] O. Kann and R. Kovács, "Mitochondria and neuronal activity," *American Journal of Physiology-Cell Physiology*, vol. 292, no. 2, pp. C641–C657, 2007. PMID: 17092996.

[38] C. V. Ly and P. Verstreken, "Mitochondria at the synapse," *The Neuroscientist*, vol. 12, no. 4, pp. 291–299, 2006. PMID: 16840705.

[39] A. Chakravorty, C. T. Jetto, and R. Manjithaya, "Dysfunctional mitochondria and mitophagy as drivers of alzheimer's disease pathogenesis," *Frontiers in Aging Neuroscience*, vol. 11, 2019.

[40] Q. Cai and Y. Y. Jeong, "Mitophagy in alzheimer's disease and other age-related neurodegenerative diseases," *Cells*, vol. 9, no. 1, 2020.

[41] Y. Wang, N. Liu, and B. Lu, "Mechanisms and roles of mitophagy in neurodegenerative diseases," *CNS Neuroscience & Therapeutics*, vol. 25, no. 7, pp. 859–875, 2019.

[42] X. Hou, J. O. Watzlawik, C. Cook, C.-C. Liu, S. S. Kang, W.-L. Lin, M. DeTure, M. G. Heckman, N. N. Diehl, F. S. H. Al-Shaikh, R. L. Walton, O. A. Ross, H. L. Melrose, N. Ertekin-Taner, G. Bu, L. Petrucelli, J. D. Fryer, M. E. Murray, D. W. Dickson, F. C. Fiesel, and W. Springer, "Mitophagy alterations in alzheimer's disease are associated with granulovacuolar degeneration and early tau pathology," *Alzheimer's and Dementia*, vol. 17, no. 3, pp. 417–430, 2021.

[43] J. Rieusset, "The role of endoplasmic reticulum-mitochondria contact sites in the control of glucose homeostasis: an update," *Cell Death & Disease*, vol. 9, p. 388, Mar 2018.

[44] S. Lee and K.-T. Min, "The interface between er and mitochondria: Molecular compositions and functions," *Molecules and cells*, vol. 41, p. 1000—1007, December 2018.

[45] L. K. Nutt, A. Pataer, J. Pahler, B. Fang, J. Roth, D. J. McConkey, and S. G. Swisher, "Bax and bak promote apoptosis by modulating endoplasmic reticular and mitochondrial ca²⁺ stores *," *Journal of Biological Chemistry*, vol. 277, pp. 9219–9225, Mar 2002.

[46] K. Palikaras, E. Lionaki, and N. Tavernarakis, "Coordination of mitophagy and mitochondrial biogenesis during ageing in c. elegans," *Nature*, vol. 521, pp. 525–528, May 2015.

[47] Y. Zheng, X. Zhang, X. Wu, L. Jiang, A. Ahsan, S. Ma, Z. Xiao, F. Han, Z. H. Qin, W. Hu, and Z. Chen, "Somatic autophagy of axonal mitochondria in ischemic neurons," *J Cell Biol*, vol. 218, pp. 1891–1907, 06 2019.

[48] N. D. Georgakopoulos, G. Wells, and M. Campanella, "The pharmacological regulation of cellular mitophagy," *Nature Chemical Biology*, vol. 13, pp. 136–146, Feb 2017.

[49] O. Yamaguchi, T. Murakawa, K. Nishida, and K. Otsu, "Receptor-mediated mitophagy," *Journal of Molecular and Cellular Cardiology*, vol. 95, pp. 50–56, Jun 2016.

[50] E. F. Fang, Y. Hou, K. Palikaras, B. A. Adriaanse, J. S. Kerr, B. Yang, S. Lautrup, M. M. Hasan-Olive, D. Caponio, X. Dan, P. Rocktäschel, D. L. Croteau, M. Akbari, N. H. Greig, T. Fladby, H. Nilsen, M. Z. Cader, M. P. Mattson, N. Tavernarakis, and V. A. Bohr, "Mitophagy inhibits amyloid-β and tau pathology and reverses cognitive deficits in models of alzheimer's disease," *Nature Neuroscience*, vol. 22, pp. 401–412, Mar 2019.

[51] A. Navarro and A. Boveris, "Brain mitochondrial dysfunction in aging, neurodegeneration, and parkinson's disease," *Frontiers in Aging Neuroscience*, vol. 2, 2010.

[52] S. Huang, X. Wang, J. Yu, Y. Tian, C. Yang, Y. Chen, H. Chen, and H. Ge, "Lonp1 regulates mitochondrial network remodeling through the pink1/parkin pathway during myoblast differentiation," *American Journal of Physiology-Cell Physiology*, vol. 319, no. 6, pp. C1020–C1028, 2020. PMID: 32936696.

[53] C. Vives-Bauza, C. Zhou, Y. Huang, M. Cui, R. L. de Vries, J. Kim, J. May, M. A. Tocilescu, W. Liu, H. S. Ko, J. Magrané, D. J. Moore, V. L. Dawson, R. Grailhe, T. M. Dawson, C. Li, K. Tieu, and S. Przedborski, "Pink1-dependent recruitment of parkin to mitochondria in mitophagy," *Proceedings of the National Academy of Sciences*, vol. 107, no. 1, pp. 378–383, 2010.

[54] S. Geisler, K. M. Holmström, D. Skujat, F. C. Fiesel, O. C. Rothfuss, P. J. Kahle, and W. Springer, "Pink1/parkin-mediated mitophagy is dependent on vdac1 and p62/sqstm1," *Nature Cell Biology*, vol. 12, pp. 119–131, Feb 2010.

[55] D. Hughes and G. R. Mallucci, "The unfolded protein response in neurodegenerative disorders – therapeutic modulation of the perk pathway," *The FEBS Journal*, vol. 286, no. 2, pp. 342–355, 2019.

[56] J. Bruch, H. Xu, T. W. Rösler, A. De Andrade, P.-H. Kuhn, S. F. Lichtenthaler, T. Arzberger, K. F. Winklhofer, U. Müller, and G. U. Höglinger, "Perk activation mitigates tau pathology in vitro and in vivo," *EMBO Molecular Medicine*, vol. 9, no. 3, pp. 371–384, 2017.

[57] S. I. Rapoport, "In vivo labeling of brain phospholipids by long-chain fatty acids: Relation to turnover and function," *Lipids*, vol. 31, pp. S97–S101, Mar 1996.

[58] G. Dhopeshwarkar, C. Subramanian, and J. F. Mead, "Metabolism of [1-14c]palmitic acid in the developing brain:persistence of radioactivity in the

carboxyl carbon," *Biochimica et Biophysica Acta (BBA) - Lipids and Lipid Metabolism*, vol. 296, no. 2, pp. 257–264, 1973.

[59] H. Tabata, J. M. Bell, J. C. Miller, and S. I. Rapoport, "Incorporation of plasma palmitate into the brain of the rat during development," *Developmental Brain Research*, vol. 29, no. 1, pp. 1–8, 1986.

[60] H. Guo, J. B. Callaway, and J. P.-Y. Ting, "Inflammasomes: mechanism of action, role in disease, and therapeutics," *Nature Medicine*, vol. 21, pp. 677–687, Jul 2015.

[61] X. shun Jiang, X. mei Chen, W. Hua, J. ling He, T. Liu, X. jia Li, J. min Wan, H. Gan, and X. gang Du, "Pink1/parkin mediated mitophagy ameliorates palmitic acid-induced apoptosis through reducing mitochondrial ros production in podocytes," *Biochemical and Biophysical Research Communications*, vol. 525, no. 4, pp. 954–961, 2020.

[62] L. Bouman, A. Schlierf, A. K. Lutz, J. Shan, A. Deinlein, J. Kast, Z. Galehdar, V. Palmisano, N. Patenge, D. Berg, T. Gasser, R. Augustin, D. Trümbach, I. Irrcher, D. S. Park, W. Wurst, M. S. Kilberg, J. Tatzelt, and K. F. Winklhofer, "Parkin is transcriptionally regulated by atf4: evidence for an interconnection between mitochondrial stress and er stress," *Cell Death & Differentiation*, vol. 18, pp. 769–782, May 2011.

[63] X. Zhang, Y. Yuan, L. Jiang, J. Zhang, J. Gao, Z. Shen, Y. Zheng, T. Deng, H. Yan, W. Li, W.-W. Hou, J. Lu, Y. Shen, H. Dai, W.-W. Hu, Z. Zhang, and Z. Chen, "Endoplasmic reticulum stress induced by tunicamycin and thapsigargin protects against transient ischemic brain injury," *Autophagy*, vol. 10, no. 10, pp. 1801–1813, 2014. PMID: 25126734.

[64] X.-j. Dai, N. Li, L. Yu, Z.-y. Chen, R. Hua, X. Qin, and Y.-M. Zhang, "Activation of bv2 microglia by lipopolysaccharide triggers an inflammatory reaction in pc12 cell apoptosis through a toll-like receptor 4-dependent pathway," *Cell Stress and Chaperones*, vol. 20, pp. 321–331, Mar 2015.

[65] T. M. Piers, E. East, C. Villegas-Llerena, I. G. Sevastou, M. Matarin, J. Hardy, and J. M. Pocock, "Soluble fibrinogen triggers non-cell autonomous

er stress-mediated microglial-induced neurotoxicity," *Frontiers in Cellular Neuroscience*, vol. 12, 2018.

[66] C. Urso and H. Zhou, "Palmitic acid lipotoxicity in microglia cells is ameliorated by unsaturated fatty acids," *International Journal of Molecular Sciences*, vol. 22, no. 16, 2021.

[67] B. Aşkın, *Assessment of the impacts of hyperlipidemia on brain and modulation of PERK pathway against hyperlipidemia-induced synaptic impairment on hippocampus*. M.S. Thesis, METU, Ankara, Turkey, July 2019.

[68] A. Fani Maleki and S. Rivest, "Innate immune cells: Monocytes, monocyte-derived macrophages and microglia as therapeutic targets for alzheimer's disease and multiple sclerosis," *Frontiers in Cellular Neuroscience*, vol. 13, 2019.

[69] Q. Escoula, S. Bellenger, M. Narce, and J. Bellenger, "Docosahexaenoic and eicosapentaenoic acids prevent altered-muc2 secretion induced by palmitic acid by alleviating endoplasmic reticulum stress in ls174t goblet cells," *Nutrients*, vol. 11, no. 9, 2019.

[70] E. Baldi and C. Bucherelli, "The inverted "u-shaped" dose-effect relationships in learning and memory: modulation of arousal and consolidation," *Nonlinearity Biol Toxicol Med*, vol. 3, pp. 9–21, Jan 2005.

[71] R. A. Gottlieb and A. Stotland, "Mitotimer: a novel protein for monitoring mitochondrial turnover in the heart," *Journal of molecular medicine (Berlin, Germany)*, vol. 93, pp. 271–278, Mar 2015.

[72] M. E. Chevreul, *A chemical study of oils and fats of animal origin*. AOCS Press, 2009.

[73] P. T. Jain and J. T. Pento, "A vehicle for the evaluation of hydrophobic compounds in cell culture," *Res Commun Chem Pathol Pharmacol*, vol. 74, pp. 105–116, Oct 1991.

[74] S. J. Marciniak, C. Y. Yun, S. Oyadomari, I. Novoa, Y. Zhang, R. Jungreis, K. Nagata, H. P. Harding, and D. Ron, "Chop induces death by promoting protein synthesis and oxidation in the stressed endoplasmic reticulum," *Genes and development*, vol. 18, pp. 3066–3077, Dec 2004.

[75] S. C. B. R. Nakandakari, V. R. Muñoz, G. K. Kuga, R. C. Gaspar, M. R. Sant'Ana, I. C. B. Pavan, L. G. S. da Silva, A. P. Morelli, F. M. Simabuco, A. S. R. da Silva, L. P. de Moura, E. R. Ropelle, D. E. Cintra, and J. R. Pauli, "Short-term high-fat diet modulates several inflammatory, er stress, and apoptosis markers in the hippocampus of young mice," *Brain, Behavior, and Immunity*, vol. 79, pp. 284–293, 2019.

[76] T. Mosmann, "Rapid colorimetric assay for cellular growth and survival: Application to proliferation and cytotoxicity assays," *Journal of Immunological Methods*, vol. 65, no. 1, pp. 55–63, 1983.

[77] S. Rose, R. E. Frye, J. Slattery, R. Wynne, M. Tippett, O. Pavliv, S. Melnyk, and S. J. James, "Oxidative stress induces mitochondrial dysfunction in a subset of autism lymphoblastoid cell lines in a well-matched case control cohort," *PLOS ONE*, vol. 9, pp. 1–16, 01 2014.

[78] I. Irrcher, P. J. Adhihetty, A.-M. Joseph, V. Ljubicic, and D. A. Hood, "Regulation of mitochondrial biogenesis in muscle by endurance exercise," *Sports Medicine*, vol. 33, pp. 783–793, Sep 2003.

[79] J. Wu, J. L. Ruas, J. L. Estall, K. A. Rasbach, J. H. Choi, L. Ye, P. Boström, H. M. Tyra, R. W. Crawford, K. P. Campbell, D. T. Rutkowski, R. J. Kaufman, and B. M. Spiegelman, "The unfolded protein response mediates adaptation to exercise in skeletal muscle through a pgc-1α/atf6α complex.," *Cell metabolism*, vol. 13, pp. 160–9, Jul 2010.

[80] C. Ruberti, E. Barizza, M. Bodner, N. La Rocca, R. De Michele, F. Carimi, F. Schiavo, and M. Zottini, "Mitochondria change dynamics and morphology during grapevine leaf senescence," *PloS one*, vol. 9, p. e102012, 07 2014.

[81] G. C. de Paula, H. S. Brunetta, D. F. Engel, J. M. Gaspar, L. A. Velloso, D. Engblom, J. de Oliveira, and A. F. de Bem, "Hippocampal function

is impaired by a short-term high-fat diet in mice: Increased blood–brain barrier permeability and neuroinflammation as triggering events," *Frontiers in Neuroscience*, vol. 15, 2021.

[82] A. K. Beery, "Inclusion of females does not increase variability in rodent research studies," *Current opinion in behavioral sciences*, vol. 23, pp. 143–149, Oct 2018.

[83] B. J. Prendergast, K. G. Onishi, and I. Zucker, "Female mice liberated for inclusion in neuroscience and biomedical research," *Neuroscience & Biobehavioral Reviews*, vol. 40, pp. 1–5, 2014.

[84] R. M. Shansky, "Are hormones a "female problem" for animal research?," *Science*, vol. 364, no. 6443, pp. 825–826, 2019.

[85] R. Hodeify, J. Megyesi, A. Tarcsafalvi, H. I. Mustafa, N. S. Hti Lar Seng, and P. M. Price, "Gender differences control the susceptibility to er stress-induced acute kidney injury," *American Journal of Physiology-Renal Physiology*, vol. 304, no. 7, pp. F875–F882, 2013.

[86] M. E. Rosa-Caldwell, S. Lim, W. S. Haynie, J. L. Brown, D. E. Lee, K. R. Dunlap, L. T. Jansen, T. A. Washington, M. P. Wiggs, and N. P. Greene, "Mitochondrial aberrations during the progression of disuse atrophy differentially affect male and female mice," *Journal of Cachexia, Sarcopenia and Muscle*, vol. 12, no. 6, pp. 2056–2068, 2021.